Bioconjugate Chemistry

Article

pubs.acs.org/bc

Clickable, Hydrophilic Ligand for *fac*-$[M^{I}(CO)_3]^+$ (M = Re/^{99m}Tc) Applied in an *S*-Functionalized α-MSH Peptide

Benjamin B. Kasten,[†] Xiaowei Ma,[‡] Hongguang Liu,[‡] Thomas R. Hayes,[†] Charles L. Barnes,[§] Shibo Qi,[‡] Kai Cheng,[‡] Shalina C. Bottorff,[†] Winston S. Slocumb,[†] Jing Wang,[∥] Zhen Cheng,*[,‡] and Paul D. Benny*[,†]

[†]Department of Chemistry, Washington State University, Pullman, Washington 99164, United States

[‡]Molecular Imaging Program at Stanford (MIPS), Department of Radiology, Bio-X Program and Canary Center at Stanford for Cancer Early Detection, Stanford University, Stanford, California 94305, United States

[§]Department of Chemistry, University of Missouri, Columbia, Missouri 65211-7600, United States

[∥]Department of Nuclear Medicine, Xijing Hospital, Fourth Military Medical University, Xi'an, Shaanxi, 710032, China

Supporting Information

ABSTRACT: The copper(I)-catalyzed azide−alkyne cycloaddition (CuAAC) click reaction was used to incorporate alkyne-functionalized dipicolylamine (DPA) ligands (**1** and **3**) for *fac*-$[M^{I}(CO)_3]^+$ (M = Re/^{99m}Tc) complexation into an α-melanocyte stimulating hormone (α-MSH) peptide analogue. A novel DPA ligand with carboxylate substitutions on the pyridyl rings (**3**) was designed to increase the hydrophilicity and to decrease in vivo hepatobiliary retention of *fac*-$[^{99m}Tc^{I}(CO)_3]^+$ complexes used in single photon emission computed tomography (SPECT) imaging studies with targeting biomolecules. The *fac*-$[Re^{I}(CO)_3(\mathbf{3})]$ complex (**4**) was used for chemical characterization and X-ray crystal analysis prior to radiolabeling studies between **3** and *fac*-$[^{99m}Tc^{I}(OH_2)_3(CO)_3]^+$. The corresponding ^{99m}Tc complex (**4a**) was obtained in high radiochemical yields, was stable in vitro for 24 h during amino acid challenge and serum stability assays, and showed increased hydrophilicity by log *P* analysis compared to an analogous complex with nonfunctionalized pyridine rings (**2a**). An α-MSH peptide functionalized with an azide was labeled with *fac*-$[M^{I}(CO)_3]^+$ using both *click, then chelate* (CuAAC reaction with **1** or **3** followed by metal complexation) and *chelate, then click* (metal complexation of **1** and **3** followed by CuAAC with the peptide) strategies to assess the effects of CuAAC conditions on *fac*-$[M^{I}(CO)_3]^+$ complexation within a peptide framework. The peptides from the *click, then chelate* strategy had different HPLC t_R's and in vitro stabilities compared to those from the *chelate, then click* strategy, suggesting nonspecific coordination of *fac*-$[M^{I}(CO)_3]^+$ using this synthetic route. The *fac*-$[M^{I}(CO)_3]^+$-complexed peptides from the *chelate, then click* strategy showed >90% stability during in vitro challenge conditions for 6 h, demonstrated high affinity and specificity for the melanocortin 1 receptor (MC1R) in IC_{50} analyses, and led to moderately high uptake in B16F10 melanoma cells. Log *P* analysis of the ^{99m}Tc-labeled peptides confirmed the enhanced hydrophilicity of the peptide bearing the novel, carboxylate-functionalized DPA chelate (**10a′**) compared to the peptide with the unmodified DPA chelate (**9a′**). In vivo biodistribution analysis of **9a′** and **10a′** showed moderate tumor uptake in a B16F10 melanoma xenograft mouse model with enhanced renal uptake and surprising intestinal uptake for **10a′** compared to predominantly hepatic accumulation for **9a′**. These results, coupled with the versatility of CuAAC, suggests this novel, hydrophilic chelate can be incorporated into numerous biomolecules containing azides for generating targeted *fac*-$[M^{I}(CO)_3]^+$ complexes in future studies.

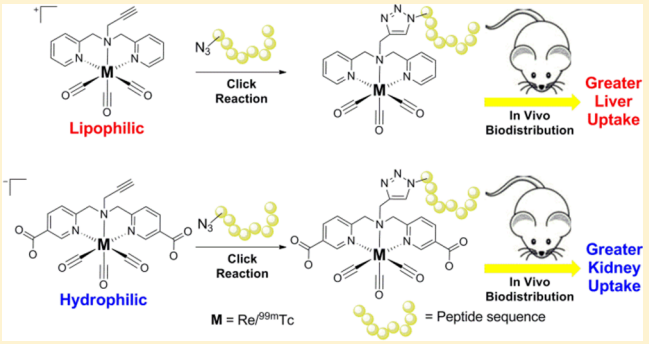

INTRODUCTION

The copper(I)-catalyzed azide−alkyne cycloaddition (CuAAC) reaction has become the icon of click chemistry since its introduction by the Sharpless and Meldal laboratories.[1,2] Numerous scientific disciplines (e.g., biology, chemical synthesis, materials science, etc.) have utilized the rapid kinetics, mild conditions, and orthogonality of CuAAC reactions for applications ranging from bioconjugation to polymer synthesis.[3−5] Methods of introducing the azide or alkyne moiety into polypeptides range from standard solid and solution phase techniques to biological incorporation using engineered codons during recombinant expression of proteins.[6−8] Due to these benefits, the number and types of biological applications using CuAAC have grown tremendously in recent years. In the field

Received: January 8, 2014
Revised: February 7, 2014
Published: February 25, 2014

   dx.doi.org/10.1021/bc5000115 | *Bioconjugate Chem.* 2014, 25, 579−592

Scheme 1. Reaction Schemes and Structures of Compounds

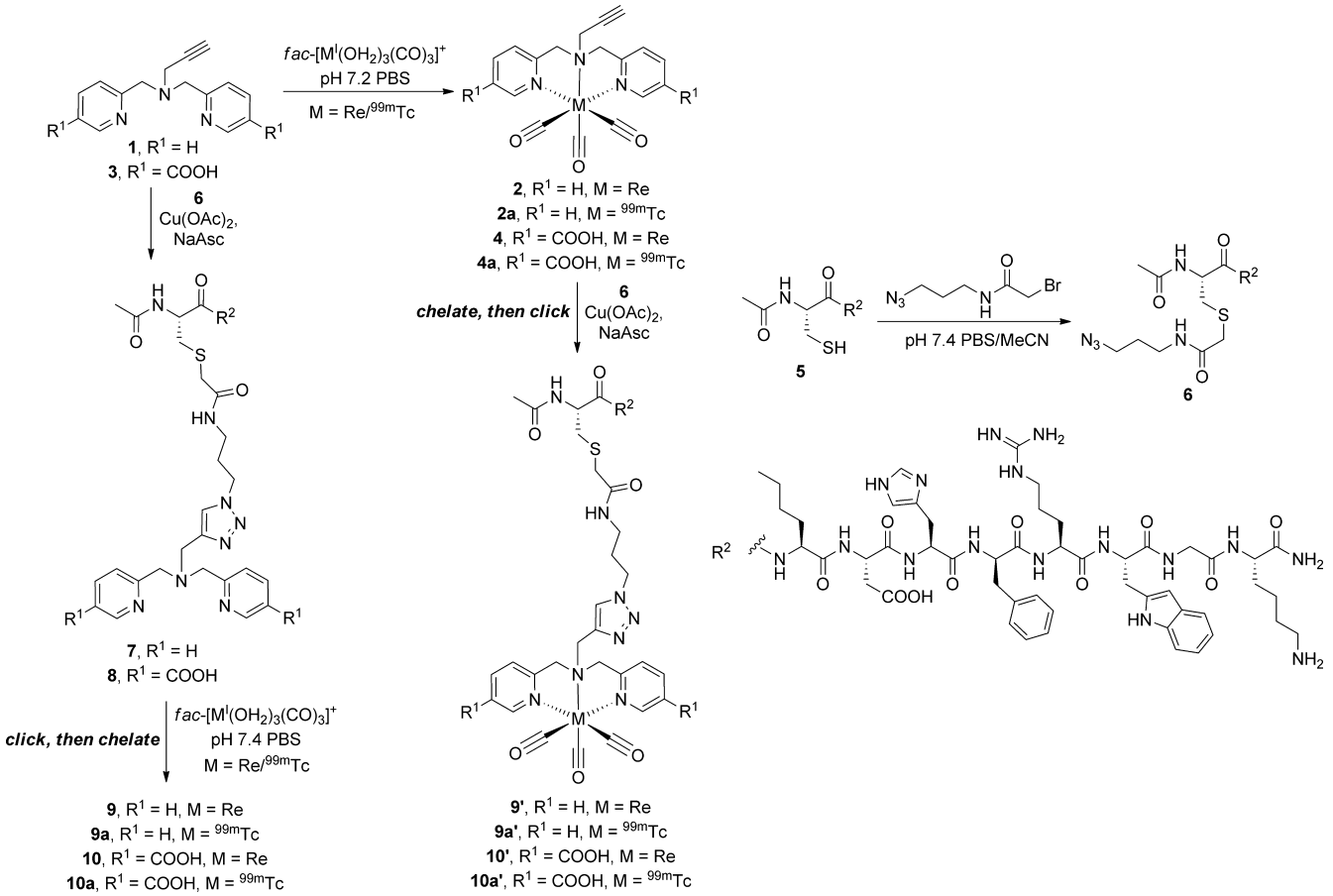

of radiopharmaceuticals, CuAAC has been harnessed for labeling a variety of biomolecules (e.g., small molecules, peptides, antibodies, etc.) with short-lived radionuclides during targeted nuclear imaging studies.[9,10] The diagnostic radionuclide ^{99m}Tc [$t_{1/2}$ = 6.02 h, 140 keV γ (89%)] has nearly ideal nuclear properties for single photon computed emission tomography (SPECT). The *fac*-[^{99m}Tc^{I}(OH$_2$)$_3$(CO)$_3$]$^+$ core developed by Alberto has gained recognition for SPECT applications due to its small molecular volume, versatile chelation chemistry, straightforward preparation from an aqueous-based kit, and amenability for readily labeling a wide variety of biomolecules.[11−14]

CuAAC has been used to incorporate ligands for the *fac*-[^{99m}Tc^{I}(CO)$_3$]$^+$ core into biomolecules by several strategies.[15] In the *click, then chelate* strategy, a biomolecule functionalized with an azide or an alkyne undergoes cycloaddition with a bifunctional chelator containing the orthogonal coupling partner prior to complexation with *fac*-[^{99m}Tc^{I}(CO)$_3$]$^+$. The *click to chelate* strategy developed by Schibli and Mindt is a variant of this method where the 1,2,3-triazole generated by the click reaction acts as an integral ligand donor for the *fac*-[^{99m}Tc^{I}(CO)$_3$]$^+$ core.[16,17] In an alternative *chelate, then click* strategy, a bifunctional chelator is first complexed with ^{99m}Tc and then joined to a biomolecule via CuAAC to generate the final radiopharmaceutical. As the click reaction can be accomplished under physiological temperature and pH, this radiolabeling strategy enables the pairing of sensitive biomolecules with ligands that require harsh labeling conditions (e.g., high temperature or pH) to drive complexation kinetics with the *fac*-[^{99m}Tc^{I}(CO)$_3$]$^+$ core.

Tridentate ligands containing aromatic nitrogen donors, such as histidine or 2,2′-dipicolylamine (DPA), have been shown to form kinetically and thermodynamically inert *fac*-[^{99m}Tc^{I}(CO)$_3$]$^+$ complexes due to the chelate effect (tridentate as opposed to mono- or bidentate ligands) and the low-spin d^6 metal center.[12,14,18−21] Despite the high in vitro and in vivo stabilities of these complexes, their formation often requires high temperatures (>90 °C) to achieve quantitative radiolabeling yields in acceptable time frames (30−60 min). Additionally, the lipophilic *fac*-[^{99m}Tc^{I}(CO)$_3$(DPA)]$^+$ complexes can lead to undesirable uptake and retention of the labeled radiopharmaceutical in nontarget tissues such as the liver and gastrointestinal tract.[22,23] In an effort to generate a versatile *fac*-[^{99m}Tc^{I}(CO)$_3$]$^+$ complex with increased hydrophilicity and high stability, we installed carboxylate groups on the aromatic rings of an alkyne-functionalized DPA ligand. Using CuAAC would allow the ligand or radiolabeled complex to be easily incorporated into a wide spectrum of targeting molecules containing an azide group. An azide-functionalized α-melanocyte stimulating hormone (α-MSH) analogue was chosen as a model targeting biomolecule to test this new chelate system with *fac*-[^{99m}Tc^{I}(CO)$_3$]$^+$.

Malignant melanoma remains the deadliest form of skin cancer due to its high metastatic rate and to challenges in detecting and treating these metastases at early stages.[24−27] Development of targeting peptides labeled with SPECT isotopes to identify metastatic melanoma at early stages

dx.doi.org/10.1021/bc5000115 | *Bioconjugate Chem.* 2014, 25, 579−592

continues to be an active area of medical research.[28−35] The majority of these peptides are α-MSH analogues which bind to the melanocortin-1 receptor (MC1R), a biomarker that is overexpressed on primary and metastatic melanoma cells (~400 to 22 000 receptors/cell) compared to normal cells.[26,36−39] Several α-MSH analogues labeled with *fac*-$[^{99m}Tc^{I}(CO)_3]^+$ have shown promising results for detecting models of melanoma in vivo during preclinical studies.[22,32,33,40−42] Utilizing various chelates and attachment strategies with α-MSH peptides has been shown to modulate the in vivo properties of the ensuing *fac*-$[^{99m}Tc^{I}(CO)_3]$-labeled peptides. While many conjugates have demonstrated undesired uptake in the liver and gastrointestinal tract,[22,32,40] introducing carboxylates on a pyrazolyl-based ligand has recently been shown to markedly reduce the hepatobiliary retention of α-MSH peptide analogues after labeling with the *fac*-$[^{99m}Tc^{I}(CO)_3]^+$ core.[33]

We hypothesized that the addition of carboxylates on a DPA chelate would increase the hydrophilicity and decrease the nonspecific hepatobiliary uptake of the resulting *fac*-$[^{99m}Tc^{I}(CO)_3]^+$ complex compared to the original DPA ligand while maintaining complex stability. To test this hypothesis, we employed a previously characterized DPA-alkyne ligand, **1**, and the new, carboxylate-functionalized DPA-alkyne ligand, **3**, in parallel studies to incorporate the *fac*-$[M^{I}(CO)_3]^+$ (M = Re/^{99m}Tc) core into an α-MSH peptide by convergent pathways (*click, then chelate* and *chelate, then click*) as shown in Scheme 1. The in vitro stabilities of the complexed ligands and peptides were determined, and the melanoma targeting potentials of the labeled peptides were evaluated through (1) in vitro MC1R affinity, (2) in vitro B16F10 cell uptake assays, and (3) in vivo biodistribution analyses in B16F10 xenograft models.

RESULTS AND DISCUSSION

In an effort to generate a versatile ligand for the *fac*-$[M^{I}(CO)_3]^+$ core with enhanced hydrophilicity, we synthesized a DPA chelate with carboxylate substitutions on the pyridal rings and a terminal alkyne on the central amine. Reductive amination between propargyl amine and methyl 6-formylnicotinate using sodium triacetoxyborohydride followed by basic hydrolysis of the methyl ester groups provided the desired ligand, **3**, in moderate overall yield (55%) following isolation and purification. Standard characterization techniques were used to confirm the structure of the isolated material as the desired compound. The IR spectrum contained a band at 3244 cm^{-1} which suggested a terminal alkyne group (CH stretching), although the corresponding expected absorption in the 2000−2200 cm^{-1} region (C≡C stretching) was not present. However, ^{1}H NMR analysis indicated the presence of a propargyl-type system due to the resonances at 3.21 and 4.06 ppm for the terminal and methylene protons, respectively. Reaction of **3** with *fac*-$[Re^{I}(OH_2)_3(CO)_3](SO_3CF_3)$ at 70 °C in mildly acidic (pH 6−6.5) aqueous conditions produced the desired complex in moderate yield (66%) following purification by preparatory RP-HPLC. As anticipated, ^{1}H NMR analysis of the isolated product, **4**, showed the methylene protons of the DPA moiety as an AB quartet (5.03/4.96 ppm) with a downfield shift from their original appearance as a singlet in the spectrum of **3** (4.62 ppm). ESI-MS analysis confirmed a ligand:$Re(CO)_3$ ratio of 1:1 in complex **4** as expected for tridentate coordination at the DPA chelate site. IR analysis indicated a facial arrangement of the carbonyls on the metal center following complexation as has been observed with other *fac*-$[Re^{I}(CO)_3(DPA)]^+$ complexes.[47,49,50]

The absolute coordination environment of **4** was confirmed through single-crystal X-ray analysis (Figure 1). Crystallographic details, bond lengths, and bond angles are given in the Supporting Information (Tables S5−S7). Crystals of **4** packed in the $P2_1/c$ space group with four molecules in the unit cell. The bond lengths and angles between the carbonyl ligands and the metal center in **4** (1.918−1.939 Å and 89.18−91.16°, respectively) were as expected for distorted octahedral *fac*-$[Re^{I}(CO)_3(DPA)]^+$ complexes.[47,49] The bond lengths between rhenium and the central nitrogen (2.227 Å) or the pyridal nitrogens (2.163 and 2.176 Å) in **4** were also similar to those in complex **2** (2.223 and 2.171 Å, respectively) as previously characterized.[47] This suggests that including the carboxylates did not significantly perturb complexation with the *fac*-$[Re^{I}(CO)_3]^+$ core. The alkyne was pointed away from the metal center as would be necessary for participation in CuAAC reactions with azides.

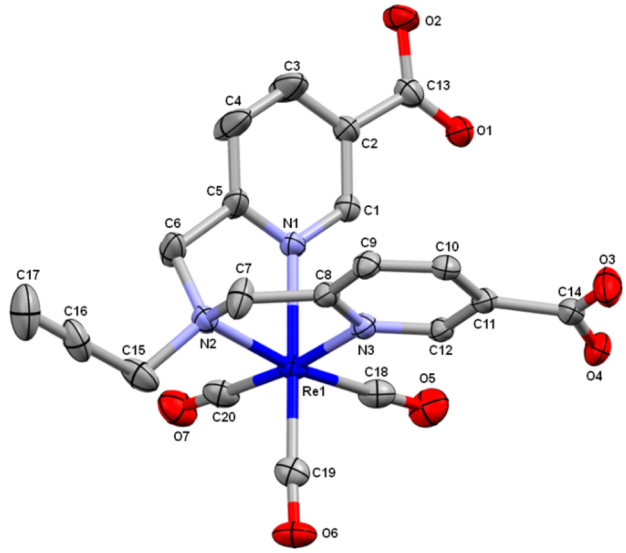

Figure 1. X-ray crystal structure of **4** with thermal ellipsoids shown at the 50% probability level. Hydrogen atoms were omitted for clarity. Atoms are colored as follows: C, gray; N, light blue; O, red; Re, dark blue.

Having established that **3** coordinates *fac*-$[Re^{I}(CO)_3]^+$ as desired, we assessed its labeling efficiency with *fac*-$[^{99m}Tc^{I}(CO)_3]^+$ to determine its potential for use in SPECT imaging applications. Radiolabeling **3** with *fac*-$[^{99m}Tc^{I}(OH_2)_3(CO)_3]^+$ at 70 °C yielded a single peak with a similar RP-HPLC t_R (19.2 min) as complex **4** (18.9 min), indicating successful formation of the desired product, **4a** (Figure 2). After determining that complexation occurred as expected, decreasing concentrations of **3** were used to examine the effects of the carboxylate substitutions on the radiolabeling efficiency compared to the original DPA-alkyne chelate, **1**. Quantitative labeling was achieved in 30 min at 70 °C when **3** was employed at 1×10^{-4} M with decreasing yields at lower concentrations (Table S1). While extending the reaction time to 1 h increased yields of **4a**, labeling efficiency with **3** was lower than with **1** to produce **2a** when identical experimental conditions were used.[47] High decay corrected yields of **4a** (>91%) could be achieved following RP-HPLC purification. A major objective in preparing the new ligand was to increase the

dx.doi.org/10.1021/bc5000115 | *Bioconjugate Chem.* 2014, 25, 579−592

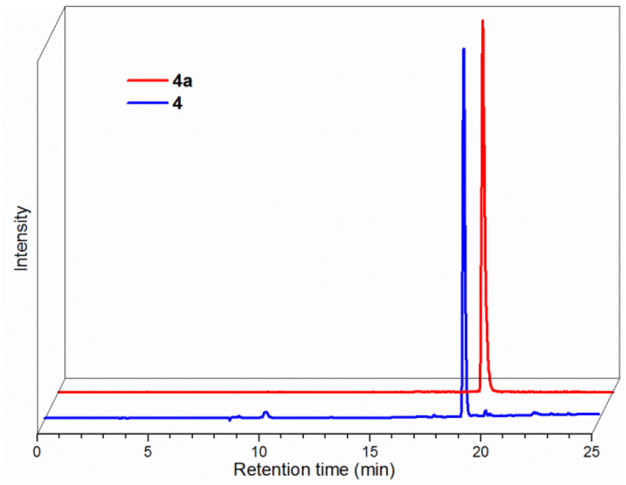

Figure 2. Normalized and offset RP-HPLC chromatograms of **4** (UV absorbance, 254 nm; lower blue trace) at t_R 18.9 min and **4a** (radiodetector, counts per minute (cpm); higher red trace) at t_R 19.2 min.

hydrophilicity of the resulting metal complex and to decrease hepatobiliary retention of radiopharmaceuticals with this complex compared to the regular DPA complex. Log *P* analysis (octanol/PBS partition coefficient) of complexes **2a** and **4a** yielded values of −0.23 ± 0.01 and −1.85 ± 0.02, respectively, confirming that the carboxylate-functionalized DPA complex was more hydrophilic than the regular DPA complex at physiological pH.

Targeted radiopharmaceuticals should maintain high biological stability with the radionuclide to avoid nonspecific uptake or retention of radioactive species in nontarget tissues during in vivo applications. Serum stability analyses and amino acid challenge assays were performed with purified solutions of **4a** to assess its resistance to transchelation or oxidation under biologically relevant conditions (Table S2). As expected from previous studies employing DPA complexes with *fac*-$[^{99m}Tc^{I}(CO)_3]^+$,[20,21,23,51] **4a** was >98% stable in serum and in the presence of 1 mM histidine or cysteine up to 24 h. These in vitro results suggested that the chelate would be suitable for further exploration within a radiopharmaceutical construct for in vivo applications.

The encouraging radiolabeling results with the novel chelate prompted its evaluation in a targeting peptide framework. A NAPamide α-MSH peptide containing a nonessential cysteine residue (Cys-NAPamide) was chosen as an initial model system to incorporate the ligand or *fac*-$[M^{I}(CO)_3]^+$ complex in a site-specific manner. NAPamide was chosen because of its high MC1R affinity and in vivo stability as demonstrated in previous studies;[39,52,53] we have recently employed a similar peptide with *fac*-$[M^{I}(CO)_3]^+$ using an alternative chelate.[41] The thiol group of cysteine presents an attractive moiety for functionalization due to its lower pK_a compared to other nucleophiles in biomolecules (e.g., amines, alcohols). Native cysteine residues are absent from many targeting biomolecules (e.g., peptides, affibodies) or are not accessible due to disulfide bridge formation (e.g., proteins, antibodies).[54,55] Therefore, synthetic or recombinant techniques can be employed to install a nonessential cysteine residue into these scaffolds for selective functionalization at locations that would not impair affinity for the biological target. Cysteine was utilized to append an azide functional group for attaching the alkyne-functionalized chelates to the peptide via CuAAC. The 2-bromo-*N*-(3-azidopropyl)-acetamide azide linker was chosen because it is stable to hydrolysis in aqueous solution, and it has previously been used for selective *S*-alkylation of proteins to incorporate an azide functionality for subsequent CuAAC reactions.[56]

The Cys-NAPamide peptide, **5**, was prepared using solid phase peptide synthesis with Fmoc-protected amino acids in high purity as indicated by RP-HPLC analysis (Figure S1). Following TCEP reduction of the peptide, alkylation was performed overnight at room temperature with a slight excess of 2-bromo-*N*-(3-azidopropyl)-acetamide in a PBS/MeCN mixture. These conditions ensured maximum alkylation of the starting peptide with minimal side product (e.g., dialkylation) formation. The alkylated peptide, **6**, was isolated in moderately high yields (>70%) and high purity (>99% by RP-HPLC, Figure S2) following RP-HPLC purification. ESI-MS analysis confirmed the identity of the product as the desired monoalkylated species (1341.1 *m*/*z*, Table 1). IR analysis showed a prominent absorption at 2103 cm^{-1} as anticipated for the presence of an azide group. Evaluation of **6** with Ellman's reagent confirmed that that the azide linker had been incorporated at the cysteine residue as no free thiols (<1%) were detected during analysis.

Following incorporation of the azide linker, two pathways were examined to label the peptide with *fac*-$[M^{I}(CO)_3]^+$: *click, then chelate* and *chelate, then click*. Both pathways have previously been utilized with DPA ligands to form metal complexes with biologically relevant small molecules through CuAAC reactions.[47,51] The *click, then chelate* route is analogous to the prevailing strategy in the literature where a targeting species is functionalized with a bifunctional chelator prior to

Table 1. Characterization Results for Non-Radioactive Peptides

		calcd MW (*m*/*z*)	obsvd MW (*m*/*z*)	RP-HPLC t_R (min)	IC_{50} (nM)
	5	$[M+2H]^{2+}$: 601.8	602.1	19.0[a]	2.19 ± 0.54
	6	$[M+2H]^{2+}$: 671.8	672.0	18.7[a]	9.60 ± 1.74
	7	$[M+2H]^{2+}$: 790.4, $[M+2H+Cu]^{2+}$: 821.9	790.7, 821.2	25.2[b]	--
	8	$[M+2H]^{2+}$: 834.4, $[M+2H+Cu]^{2+}$: 865.8	834.7, 866.2	25.7[b]	--
Click, then chelate	**9**	$[M+H]^{2+}$: 925.4	925.7	14.6[c]	--
	10	$[M+H]^{2+}$: 968.9	968.7	14.4[c]	--
Chelate, then click	**9′**	$[M+H]^{2+}$: 925.4	925.5	14.9[c]	3.57 ± 1.15
	10′	$[M-H]^{-}$: 1936.7	1936.3	15.3[c]	3.13 ± 0.29

[a]HPLC method 3. [b]HPLC method 4. [c]HPLC method 6.

dx.doi.org/10.1021/bc5000115 | *Bioconjugate Chem.* 2014, 25, 579−592

complexation with the metal. The *chelate, then click* approach was used as an alternative strategy to generate the metal-complexed peptides to determine if the presence of the *fac*-$[M^{I}(CO)_3]^+$ core prior to the CuAAC reaction affected formation of the desired products. CuAAC reactions were performed to append ligands **1** or **3** to peptide **6** in order to yield constructs **7** and **8** containing the standard DPA chelate and the new DPA chelate bearing carboxylates, respectively. Due to the likelihood of copper coordination by the DPA chelates,[51,57] excess $Cu(OAc)_2$ was used in the CuAAC reactions to ensure that enough copper(I) would be available to catalyze the desired cycloaddition reactions. After RP-HPLC analysis indicated completion of the reactions, EDTA or sodium sulfide was added to remove copper and the crude peptides were purified to a single peak by RP-HPLC (Table 1, Figures S3 and S4). ESI-MS analysis indicated that the peptides were produced as desired due to the resonances at 790.7 *m*/*z* and 834.7 *m*/*z* for the $[M+2H]^{2+}$ ions of **7** and **8**, respectively (Table 1), although copper complexes of these peptides were also apparent as minor species in the MS spectra (821.2 *m*/*z* and 866.2 *m*/*z* for $[M+2H+Cu]^{2+}$ ions of **7** and **8**, respectively, Table 1). This result is similar to what has been observed previously with the DPA-alkyne ligand, **1**, following CuAAC reaction with a functionalized azide.[51] Using excess sodium sulfide to remove residual copper from the peptides by forming CuS was only partially successful; employing precoordinated copper complexes (e.g., tris-(benzyl-triazolylmethyl)amine) during the CuAAC reactions also failed to yield **7** and **8** without residual copper present (data not shown). Despite the presence of copper in the peptides, subsequent reactions of **7** and **8** with *fac*-$[Re^{I}(OH_2)_3(CO)_3](SO_3CF_3)$ yielded the rhenium-complexed peptides **9** and **10**, respectively, following RP-HPLC purification (Figures S5 and S6). ESI-MS analysis of **9** and **10**, which showed the anticipated $[M+H]^{2+}$ ions at 925.7 *m*/*z* and 968.7 *m*/*z*, respectively, confirmed coordination of the *fac*-$[Re^{I}(CO)_3]^+$ core to the peptides (Table 1), and no copper was evident during analysis following *fac*-$[Re^{I}(CO)_3]^+$ complexation. Overall yields of **9** and **10** from the starting azide-functionalized peptide **6** via the *click, then chelate* strategy were 50% and 39%, respectively.

The *chelate, then click* route was then examined to compare overall reaction yields from **6** and to determine if the products obtained corresponded to those via the *click, then chelate* route. A particular advantage of the *chelate, then click* synthetic strategy is that the ligand is complexed with the *fac*-$[M^{I}(CO)_3]^+$ center prior to cycloaddition with the azide on the peptide, assuring that the final metal-complexed product is obtained as desired without the possibility of mixed coordination species. Surprisingly, RP-HPLC analysis of the *chelate, then click* reactions between peptide **6** and complexes **2** and **4** indicated that species with slightly different t_R's were formed compared to those from the *click, then chelate* pathway (Table 1). ESI-MS analysis of these new species, designated **9′** for the analogue with the regular DPA complex and **10′** for the analogue with the carboxylate-functionalized DPA complex, following RP-HPLC purification of the reactions confirmed that the *fac*-$[Re^{I}(CO)_3]^+$-labeled peptides were successfully obtained without residual copper via this synthetic pathway (925.5 *m*/*z* for $[M+H]^{2+}$ ions of **9′** and 1936.3 *m*/*z* for $[M-H]^-$ ions of **10′**, Table 1). Yields for **9′** and **10′** obtained by the *chelate, then click* strategy from peptide **6** were 47% and 70%, respectively. The different t_R's of **9**/**9′** and **10**/**10′** suggest that the presence of copper prior to rhenium complexation negatively affected the desired coordination of the *fac*-$[Re^{I}(CO)_3]^+$ core in the *click, then chelate* strategy. In subsequent reactions, the peptides obtained by the *chelate, then click* strategy (**9′** and **10′**) were hypothesized to possess the desired *N*,*N*,*N* coordination mode exclusively at the chelate position because metal complexation with the DPA ligands, which possess well-defined coordination and high stability with the *fac*-$[Re^{I}(CO)_3]^+$ core,[47,49,58] was performed prior to attachment to the peptide. The rhenium-complexed peptides produced by the *click, then chelate* pathway (**9** and **10**) were likely coordination isomers of the desired products and were not pursued in the biological assays below.

Peptides **5**, **6**, **9′**, and **10′** were used in B16F10 melanoma cell competitive binding assays with a standard radiolabeled MC1R binding peptide, ^{125}I-(Tyr^2)-NDP, to confirm that the modifications made to the peptides through linker attachment and metal complexation did not abrogate their affinity for the MC1R. These assays yielded IC_{50} values in the low nanomolar range for the peptides (Table 1), although the IC_{50} values were higher than that of the previously reported NAPamide sequence when tested with B16F1 melanoma cells (0.27 nM).[59] The high affinity of the metalated analogues supported further exploration of the peptides with ^{99m}Tc for targeting melanoma in SPECT applications.

Both synthetic pathways used with the rhenium analogues were explored for producing the ^{99m}Tc-complexed peptides. In the *click, then chelate* pathway, peptides **7** and **8** containing the DPA chelate and the carboxylate-functionalized DPA chelate, respectively, were directly complexed with *fac*-$[^{99m}Tc^{I}(OH_2)_3(CO)_3]^+$ at 70 °C for 1 h in PBS. RP-HPLC analysis showed similar t_R's for these ^{99m}Tc-labeled peptides, designated **9a** and **10a** (Table 2, Figures S5 and S6), as was

Table 2. RP-HPLC t_R's and Isolated Radiolabeling Yields of Peptides Labeled with ^{99m}Tc Following RP-HPLC Purification

	Click, then chelate		*Chelate, then click*	
	9a	**10a**	**9a′**	**10a′**
RP-HPLC t_R (min)	14.6[a]	14.4[a]	15.1[a]	15.5[a]
isolated, decay-corrected yields	84%	47%	42%	71%

[a]HPLC method 6.

observed for the respective rhenium analogues, **9** and **10** (Table 1), produced by the *click, then chelate* strategy. This suggested that similar coordination modes were obtained with both *fac*-$[M^{I}(CO)_3]^+$ cores using these peptides. Radiolabeling yields of **9a** and **10a** after 1 h at 70 °C were greater than 93% (conversion from *fac*-$[^{99m}Tc^{I}(OH_2)_3(CO)_3]^+$) when the peptides were used at ~5 × 10^{-5} M with declining yields at shorter times and lower concentrations as was observed with the ligands (**1** and **3**) before attachment to the peptides. Purification of the products by RP-HPLC yielded **9a** and **10a** in moderate decay-corrected yields (Table 2).

The *chelate, then click* pathway was next explored to produce the ^{99m}Tc-complexed peptides **9a′** and **10a′**. Performing the CuAAC reactions with ~5 × 10^{-5} M **6** and crude reaction mixtures of **2a** or **4a** at 50 °C in PBS yielded **9a′** and **10a′** quantitatively (>98% conversion from **2a** or **4a**) in as little as 30 min, although decay-corrected yields of **9a′** and **10a′** were moderate following RP-HPLC isolation (Table 2). Comparison of the RP-HPLC t_R's of the Re and ^{99m}Tc analogues produced by the *chelate, then click* route validated the identities of **9a′** and **10a′** (Tables 1 and 2, Figures 3 and 4). As was observed with

dx.doi.org/10.1021/bc5000115 | *Bioconjugate Chem.* 2014, 25, 579−592

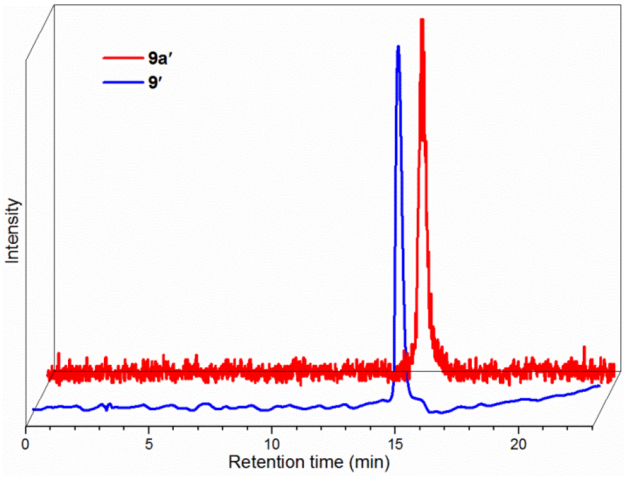

Figure 3. Normalized and offset RP-HPLC chromatograms of **9′** (UV absorbance, 220 nm; lower blue trace) at t_R 14.9 min and **9a′** (radiodetector, counts per minute (cpm); higher red trace) at t_R 15.1 min produced by the *chelate, then click* route.

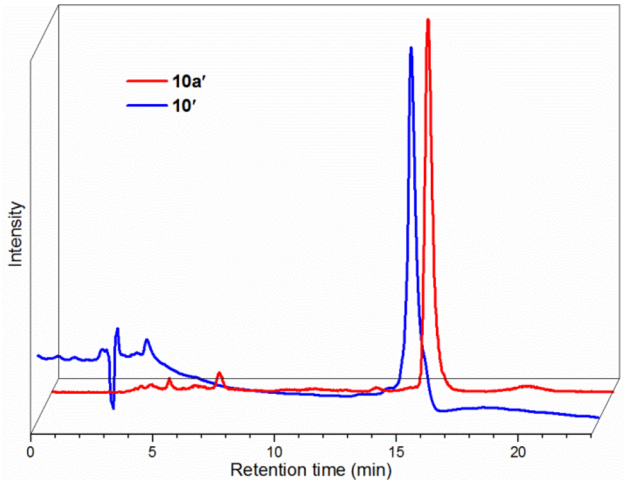

Figure 4. Normalized and offset RP-HPLC chromatograms of **10′** (UV absorbance, 238 nm; earlier blue trace) at t_R 15.3 min and **10a′** (radiodetector, counts per minute (cpm); later red trace) at t_R 15.5 min produced by the *chelate, then click* route.

the rhenium-complexed peptides, different RP-HPLC t_R's of **9a**/**9a′** and **10a**/**10a′** were observed for the products of the *chelate, then click* route compared to the *click, then chelate* route (Table 2).

The in vitro stabilities of the radiolabeled peptides were examined prior to testing their in vivo properties. It was likely that the stabilities of **9a** and **10a** would differ from **9a′** and **10a′** due to the potentially different *fac*-$[^{99m}Tc^{I}(CO)_3]^+$ coordination modes resulting from the *click, then chelate* and *chelate, then click* strategies. Peptide **9a′** was >99% stable in the presence of either histidine or cysteine at 37 °C for 4 h with slightly lower stability (84%) in cysteine at 18 h (Table S3). Peptide **10a′** exhibited >99% stability under these conditions for 18 h (Table S3). Both **9a′** and **10a′** were >90% stable for 6 h at 37 °C in serum (Table S4) which indicated they would be candidates for further biological analysis. RP-HPLC analysis of **9a** and **10a** produced via the *click, then chelate* route, however, showed multiple species at times beyond 2 h in the above challenge conditions and when incubated in PBS at room temperature following purification (data not shown). This suggests that residual copper which was apparent in peptides **7** and **8** prior to complexation with the *fac*-$[^{99m}Tc^{I}(CO)_3]^+$ core led to less stable coordination modes or may have negatively impacted the integrity of the radiolabeled peptides (e.g., through metal-mediated peptide hydrolysis[60,61]). Employing the precomplexed ligands in the *chelate, then click* strategy did not suffer these drawbacks, thus highlighting the benefit of this synthetic pathway for generating the desired *fac*-$[^{99m}Tc^{I}(CO)_3]^+$-complexed peptides, **9a′** and **10a′**. Having determined which species were stable in solution, the effects of the two chelates (regular DPA vs carboxylate-functionalized DPA) on the overall hydrophilicity of the peptides was examined. Under the acidic conditions (0.1% TFA) used for RP-HPLC analysis, the analogues bearing the novel chelate (**8**, **10′**, **10a′**) had slightly longer t_R's compared to their counterparts with the unmodified DPA chelate (**7**, **9′**, **9a′**). This observation could be explained by protonation of one of the carboxylates on the modified DPA chelate at low pH, leading to a zwitterionic form of the chelate in **8** and an overall neutral charge for the metal complexes in **10′** and **10a′**. The DPA ligand in **7**, on the other hand, was protonated at low pH; complexation with the metal in **9′** and **9a′** retained the positive charge from the *fac*-$[M^{I}(CO)_3]^+$ core regardless of pH. Thus, the t_R's of the compounds under the acidic RP-HPLC conditions did not adequately correlate to the anticipated hydrophilicity of the compounds at physiological pH. Log *P* analysis at neutral pH confirmed the increased hydrophilicity of **10a′** (−2.03 ± 0.01) compared to **9a′** (−0.68 ± 0.04) as would be desired for generating a targeted peptide with less hepatobiliary retention compared to the more hydrophobic analogue.

Following the radiolabeling and characterization studies above, the in vitro B16F10 melanoma cell uptake and MC1R specificity of **9a′** and **10a′** were explored at 0.5, 1, and 2 h (Figure 5). **9a′** exhibited moderate accumulation in B16F10 melanoma cells at 37 °C, reaching 2.71 ± 0.18%, 3.30 ± 0.44%, and 5.86 ± 1.07% of applied activity at 0.5, 1, and 2 h,

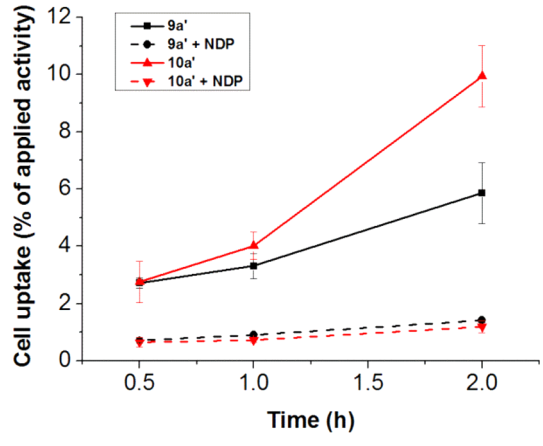

Figure 5. In vitro B16F10 cell uptake assay of **9a′** and **10a′**. B16F10 cells were incubated with 1 μCi of **9a′** or **10a′** for 0.5, 1, and 2 h at 37 °C with or without NDP (3 μM) as a blocking agent. Data represent the amount of activity associated with the cells as a percentage of the total activity applied ± standard deviation and are the average of two individual experiments performed in quadruplicate. **9a′** only (black squares with solid black line), **9a′** with NDP (black circles with dotted black line), **10a′** only (red triangles with solid red line), and **10a′** with NDP (red triangles with dotted red line).

dx.doi.org/10.1021/bc5000115 | *Bioconjugate Chem.* 2014, 25, 579−592

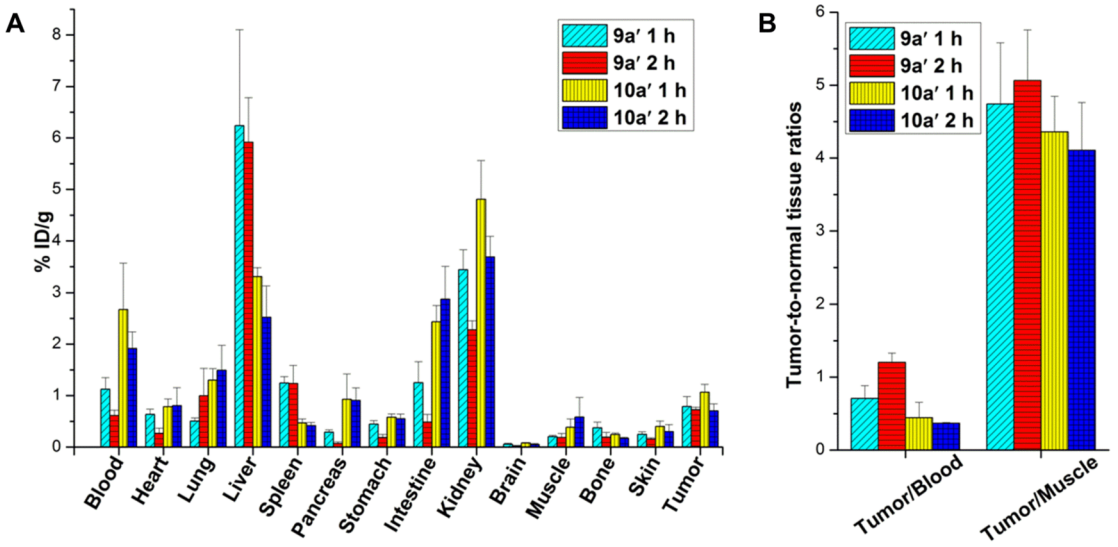

Figure 6. Biodistribution (A) and tumor-to-normal tissue ratios (B) of **9a′** and **10a′** in B16F10 tumor-bearing C57BL/6 mice 1 and 2 h after injection of approximately 100 μCi of **9a′** and **10a′** via the tail vein. Data are expressed as % ID/g ± standard deviation (n = 4 per group).

respectively. Interestingly, increased cell uptake values were observed for **10a′**, reaching 2.75 ± 0.72%, 4.01 ± 0.47%, and 9.40 ± 1.08% at 0.5, 1, and 2 h, respectively. The significantly higher uptake of **10a′** compared to **9a′** at 2 h ($P < 0.05$) in the melanoma cells was surprising considering that the rhenium-complexed analogues exhibited similar IC_{50} values in the MC1R binding assays (3.57 ± 1.15 nM for **9′** and 3.13 ± 0.29 for **10′**). To confirm whether the binding of **9a′** and **10a′** with B16F10 cells was due to specific interactions with MC1R, the cells were coincubated with solutions containing **9a′** or **10a′** and excess amounts of unlabeled NDP for 0.5, 1, and 2 h at 37 °C. As shown in Figure 5, these blocking conditions caused a decrease in the uptake of the radiolabeled peptides at 2 h from 5.86 ± 1.07% to 1.42 ± 0.08% ($P < 0.05$) for **9a′** and from 9.40 ± 1.08% to 1.20 ± 0.22% ($P < 0.05$) for **10a′**. Thus, unlabeled NDP significantly reduced the binding of **9a′** and **10a′** to B16F10 cells, indicating that the uptake of the radiolabeled peptides was mediated by the MC1R.

The above in vitro stability and cell uptake results encouraged the investigation of **9a′** and **10a′** as potential SPECT peptides for targeting melanoma in vivo. The biodistribution patterns of **9a′** and **10a′** were examined in B16F10 melanoma mouse xenograft models at 1 and 2 h to quantify the uptake of these peptides following intravenous administration. The results are presented in Figure 6. Peptide **9a′** accumulated to the greatest extent in the liver and kidneys (5.92 ± 0.87% and 2.28 ± 0.18% at 2 h p.i., respectively), although retention in the spleen and lung was also observed at 2 h p.i. (1.24 ± 0.35% and 1.00 ± 0.53%, respectively). Other peptides and small molecule targeting ligands with *fac*-$[^{99m}Tc(CO)_3(DPA)]^+$ complexes have shown similar biodistribution patterns with high uptake in the hepatobiliary system.[23,62−64] Using the carboxylate-substituted DPA complex in peptide **10a′** was anticipated to decrease the hepatobiliary retention of this analogue relative to **9a′** due to the increased hydrophilicity of the novel chelate. Compared to **9a′**, peptide **10a′** exhibited greater renal (3.69 ± 0.40%) than hepatic (2.52 ± 0.61%) accumulation at 2 h p.i.; retention of **10a′** in the blood (1.91 ± 0.33%), lung (1.50 ± 0.48%), pancreas (0.91 ± 0.25%), and intestine (2.87 ± 0.63%) was also higher compared to **9a′** at 2 h p.i. (0.61 ± 0.10%, 1.00 ± 0.53%, 0.07 ± 0.03%, and 0.49 ± 0.15% for blood, lung, pancreas, and intestine, respectively). The different accumulations of **9a′** and **10a′** observed in the liver and kidneys confirmed that incorporation of the carboxylates on the DPA complex in **10a′** altered the properties of the resulting radiopharmaceutical in vivo compared to the original DPA complex in **9a′**. However, the amount of **10a′** observed in the intestines suggests the desired goal of decreasing hepatobiliary retention by using the hydrophilic complex was not achieved. The lower level of **9a′** in the intestines at 2 h (0.49 ± 0.15%) compared to **10a′** (2.87 ± 0.63%) suggests that the carboxylate substitutions may have increased the rate of clearance through the liver without significantly modifying total hepatobiliary uptake. Although the greater levels of **10a′** in the kidneys and in the blood and could be due to its increased hydrophilicity (compared to **9a′**), prolonged blood retention of the radionuclide using this analogue would adversely affect signal-to-noise ratios of MC1R-expressing tissues during SPECT imaging.

The two different chelates did not appear to affect MC1R affinity in vivo as tumor uptake was comparable for both peptides, reaching 0.79 ± 0.19% for **9a′** and 1.06 ± 0.16% for **10a′** at 1 h p.i. and declining to 0.73 ± 0.05% for **9a′** and 0.71 ± 0.14% for **10a′** at 2 h p.i. The tumor-to-blood ratio (Figure 6) slightly increased for **9a′** at 2 h p.i. (1.2 ± 0.13) compared to 1 h p.i. (0.7 ± 0.17) as would be desired for obtaining SPECT images of target tissues with low background levels at later time points. Although the amount of **10a′** in the blood also decreased over time, its higher overall blood retention led to lower tumor-to-blood ratios (~0.4 at both 1 and 2 h p.i.) compared to **9a′**. Many tissues (stomach, brain, muscle, bone, skin) exhibited lower uptake and retention of **9a′** and **10a′** compared to the melanoma tumors (Figure 6) as would be desired for diagnostic imaging of malignant melanoma. However, due to the rates of melanoma metastases in the hepatobiliary and gastrointestinal systems,[65] additional modifications to **9a′** and **10a′** would be required to minimize the nonspecific retention of these peptides in soft tissues prior to further development in SPECT imaging applications.

A variety of chelates for the *fac*-$[M^I(CO)_3]^+$ core have been designed with modifications to increase the hydrophilicity and renal clearance of the resulting complexes.[21,23,33,64,66] Several

dx.doi.org/10.1021/bc5000115 | *Bioconjugate Chem.* 2014, 25, 579−592

have employed the single amino acid chelate (SAAC) approach which is useful for inserting ligands at nearly any desired location in peptides made by solid phase synthesis.[21,23,58] Pyrazolyl chelates modified with carboxylate groups have also been employed in α-MSH peptides for targeting melanoma.[33] Both strategies have successfully produced peptides with lower soft tissue retention and greater excretion through renal rather than hepatobiliary pathways compared to unmodified chelate structures. The DPA chelates used in the present study were intended to build on the above concepts by employing a versatile linker strategy that could be utilized with peptides or even larger macromolecules produced by both synthetic and recombinant techniques. Such techniques could be used to insert azide-bearing residues (or orthogonal reactive groups for selectively incorporating azides) for chelate attachment via CuAAC at potentially at any location in the sequence of the biomolecule, thus promoting the flexibility of the chelation strategy used here compared to the other strategies mentioned above.

While the chelates and CuAAC strategies used here are expected to be generally applicable for labeling biomolecules with the *fac*-$[M^{I}(CO)_3]^+$ core, several limitations are worth noting. First, it is possible that incorporating modified residues within highly optimized targeting ligands (e.g., small molecules, short peptides) could negatively affect their binding affinities or pharmacokinetic properties compared to the original targeting moiety. Second, the unstable nature of the metal-complexed α-MSH peptides generated through the *click, then chelate* route in this study suggests that residual Cu from the CuAAC reaction can potentially lead to undefined *fac*-$[M^{I}(CO)_3]^+$ complexes during applications with complex biomolecules. This drawback, along with other limitations associated with CuAAC click reactions (e.g., purification requirements to avoid Cu toxicity, transchelation, etc.) must be considered during future applications with the *click, then chelate* strategy in particular. Additionally, using the carboxylate-modified DPA complex with the α-MSH peptide in the present study did not lead to the desired decrease in hepatobiliary retention compared to the unmodified DPA complex. Despite these observations, the hydrophilic ligand for the *fac*-$[M^{I}(CO)_3]^+$ core in the *chelate, then click* strategy confirmed that its incorporation into a targeting peptide did not significantly impair peptide function when compared with a known DPA complex containing the *fac*-$[M^{I}(CO)_3]^+$ core. The *chelate, then click* strategy prevents the possibility of undefined or unstable coordination isomers of the metal core at undesired sites in targeting biomolecules and can allow even temperature-sensitive biomolecules to be rapidly labeled with the *fac*-$[M^{I}(CO)_3]^+$ core under mild conditions.[47] Therefore, utilizing this strategy with either of the metal complexes from the present study would be suitable for generating a wide variety of targeting radiopharmaceuticals in future applications.

CONCLUSIONS

In summary, a novel chelate based on DPA with enhanced hydrophilicity has been developed and utilized with the *fac*-$[M^{I}(CO)_3]^+$ core. Structural assessment using Re and radiolabeling studies with ^{99m}Tc demonstrated that this chelate's performance was comparable to a well characterized DPA ligand. An α-MSH analogue with an *S*-functionalized azide linker was used as a model biomolecule to incorporate the alkyne-functionalized chelates and *fac*-$[M^{I}(CO)_3]^+$ complexes into the peptides via CuAAC reactions. Metal complexation through the *click, then chelate* route produced peptides with inferior in vitro properties compared to those generated by the *chelate, then click* strategy. The *fac*-$[M^{I}(CO)_3]^+$-complexed analogues generated by the *chelate, then click* strategy were stable to transchelation, possessed high affinity for the MC1R, and demonstrated encouraging uptake values in B16F10 melanoma cells in vitro. Biodistribution analysis of the peptides bearing the two different DPA chelates demonstrated moderately low uptake in melanoma xenografts in vivo. While the α-MSH peptide with the new carboxylate-functionalized complex showed slightly increased renal accumulation and less hepatic retention than the alternative hydrophobic analogue, the desired goal of decreasing hepatobiliary retention by increasing the hydrophilicity of this analogue was not obtained. However, the versatility of the *chelate, then click* strategy with either of the chelates used here maintains the potential to incorporate the *fac*-$[M^{I}(CO)_3]^+$ core into a wide variety of biomolecules bearing azide moieties for generating targeted radiopharmaceuticals via CuAAC.

EXPERIMENTAL PROCEDURES

All reagents and solvents were of reagent grade or higher from commercial suppliers (Aldrich, Fluka, Acros, Fisher) and used as received unless noted otherwise. *fac*-$[Re^{I}(OH_2)_3(CO)_3](SO_3CF_3)$,[43] methyl 6-formylnicotinate,[44] 2-bromo-*N*-(3-azidopropyl)-acetamide,[45] *N*,*N*-bis(pyridine-2-ylmethyl)prop-2-yn-1-amine[46] (ligand **1**), and *fac*-$[Re^{I}(CO)_3(\mathbf{1})](SO_3CF_3)$[47] (complex **2**) were prepared from literature procedures. $[^{99m}TcO_4]^-$ was obtained from Cardinal Health (Spokane, WA) or from Stanford Nuclear Medicine Clinic and was used to prepare *fac*-$[^{99m}Tc^{I}(OH_2)_3(CO)_3]^+$ via commercially available Isolink kits (Tyco, Inc.) as previously described.[41] ^{125}I-(Tyr^2)-[Nle^4,D-Phe^7]-α-MSH [^{125}I-(Tyr^2)-NDP] was purchased from Perkin-Elmer (Waltham, MA). Rink Amide LS resin, hydroxybenzotriazole (HOBt), and 9-fluorenylmethoxycarbonyl (Fmoc) protected amino acids were purchased from Advanced ChemTech (Louisville, KY). Elemental analysis was performed by Intertek Pharmaceutical Services, Inc. (Whitehouse, NJ). Nuclear magnetic resonance (NMR) spectra were recorded at 293 K on 300 or 400 MHz Varian Mercury Vx spectrometers using 5 mm NMR tubes. ^{1}H and ^{13}C NMR spectra peak positions were referenced using residual solvent signals, and spectra were processed using Varian VNWR 6.1 software. Mass spectra were obtained on a Thermo-Finnigan LCQ Advantage instrument for electrospray ionization mass spectrometry (ESI-MS). Infrared (IR) spectra were recorded on a Thermo Nicolett 6700 FTIR with an ATR cell and analyzed with OMNIC 7.1a software. UV/vis spectra were recorded on a Varian Cary 50 Bio spectrophotometer and analyzed with Cary WinUV 3.00 software. Solutions of the compounds were prepared in UV/vis quality methanol and measured in 1 cm path length quartz cuvettes. Analytical separation and identification of small molecules and peptides by reversed-phase high performance liquid chromatography (RP-HPLC) were conducted using a Varian Pursuit XRs column (C18, 5 μm, 4.6 × 250 mm) with a Phenomenex security guard cartridge (C18, 4.0 × 3.0 mm). A Perkin-Elmer Series 200 analytical chromatography system equipped with a Perkin-Elmer Radiomatic 610TR detector and a Hitachi D-7000 series analytical chromatography system (L-7100 pump, L-7400 UV detector) equipped with a Berthold FlowStar LB 513 radiodetector were used for the above compounds. Unless noted otherwise, elutions performed on these systems used a

dx.doi.org/10.1021/bc5000115 | Bioconjugate Chem. 2014, 25, 579−592

gradient profile (HPLC method 1, previously described as "Gradient 1")[48] with 0.1% TFA in water (solvent A) and MeOH (solvent B) as solvents. Chromatograms were plotted using OriginPro 8.5.1 (OriginLab Corporation, MA). Preparatory RP-HPLC separations and purifications of small molecules used a Phenomenex Gemini-NX column (C18, 5 μm, 21.2 × 250 mm) with a Phenomenex security guard cartridge (C18, 21.2 × 15 mm) on a Hitachi D-7000 series semipreparative chromatography system (L-7150 pump, L-7400 UV detector). Chromatographic analysis and purification of the starting peptide (**5**; Scheme 1) was performed on a Dionex Ultimate 300 HPLC system (Dionex Corp.) using both semipreparative (Vydac; 218TP510-C18, 5 μm, 10 × 250 mm) and analytic (Vydac; 214TP54-C18, 5 μm, 4.6 × 250 mm) peptide RP-HPLC columns. The mobile phase gradients used 0.1% TFA in water (solvent A) and 0.1% TFA in acetonitrile (MeCN, solvent C). Radio-HPLC purification and analysis with the radiolabeled peptides used for biological analysis (**9a′** and **10a′**; Scheme 1) was conducted with a semipreparative RP-HPLC Vydac peptide column on a Dionex 680 chromatography system with a UVD 170U absorbance detector and model 105S single-channel radiation detector (Carroll & Ramsey Associates, Berkley, CA) using a gradient method (HPLC method 2: 1 mL/min flow rate; 0−3 min 95% A/5% C, 3−8 min linear gradient to 72% A/28% C, 8−33 min linear gradient to 67% A/33% C, 33−36 min linear gradient to 5% A/95% C, 36−39 min hold 5% A/95% C, return to 95% A/5% C after 39 min and equilibrate). The recorded data were processed with use of Chromeleon v 6.50 software (Sunnyvale, CA) and were plotted using Origin 8.0 (MicroCal). The B16F10 murine melanoma cell line was obtained from American Type Culture Collection (Manassas, VA). Female C57BL/6 mice were purchased from Charles River Laboratory (Wilmington, MA).

Small Molecule Synthesis and Complexation Reactions. *6,6′-((Prop-2-yn-1-ylazanediyl)bis(methylene))-dinicotinic Acid, **3**.* Methyl 6-formylnicotinate (0.250 g, 1.514 × 10^{-3} mol) was dissolved in 1,2-dichloroethane (10 mL) while stirring under N_2. Propargyl amine (0.042 mL, 6.58 × 10^{-4} mol) was added followed by sodium triacetoxyborohydride (0.349 g, 1.645 × 10^{-3} mol) and the resulting mixture was stirred for 3 h. Water (10 mL) was added to quench the reaction and the solution was stirred for an additional 5 min. The solution was diluted with 20 mL CH_2Cl_2 and 20 mL 1 M NaOH. The organic layer was collected and the aqueous layer was washed with CH_2Cl_2 (2 × 20 mL). The combined organic layers were dried with $MgSO_4$, filtered, and concentrated to dryness. The resulting yellow oil was dissolved in MeOH and a 1 M solution of NaOH (0.724 mL, 7.24 × 10^{-4} mol) was added. The reaction was heated to reflux for 2 h and then concentrated to dryness under vacuum. The crude residue was redissolved in H_2O and brought to pH 2−3 with 1 M HCl. The precipitate that formed during acidification was collected by filtration and rinsed with ice-cold H_2O to yield 41.3 mg of the desired product. The remaining filtrate was purified by preparatory RP-HPLC using a gradient method (prep-HPLC method 1) with the following conditions: 10 mL/min flow rate; 0−3 min 100% A, 3−9 min 75% A/25% B, 9−25 min linear gradient to 100% B, 25−32 min 100% B, 32−33 min linear gradient to 100% A, 33−38 min equilibrate in 100% A; UV at 220 nm. Product peak t_R: 20.6 min. Purified portions were combined and concentrated to dryness under vacuum to yield an additional 104 mg of the desired product as a brown powder. Combined yield, 55%. Anal. Calcd for $C_{17}H_{15}N_3O_4 \cdot 2.25$ HCl: C, 50.12; H, 4.27; N, 10.32. Found: C, 50.05; H, 3.61; N, 10.06. ^{1}H NMR [δ (ppm), 400 MHz, CD_3OD]: 9.20 (d, $C_{Py}H$, 2 H), 8.50 (dd, $C_{Py}H$, 2 H), 7.72 (d, $C_{Py}H$, 2 H), 4.62 (s, Py-CH_2-N, 4 H), 4.06 (d, N-CH_2-C, 2 H), 3.21 (dd, CC*H*, 1 H). ^{13}C NMR [δ (ppm), 100 MHz, D_2O]: 164.9 (COO), 155.4 (Ar-C), 146.2 (d, 32.8 Hz, Ar-C), 143.7 (d, 28.8 Hz, Ar-C), 129.4 (Ar-C), 127.0 (t, 36.2 Hz, Ar-C), 76.8 (d, 73.2 Hz, N-CH_2), 75.6 (d, 14.8 Hz, N-CH_2), 55.0 (t, 25.7 Hz, CH_2-C≡CH), 42.6 (t, 14.1 Hz, C≡*C*H). MS (+ESI): 326.1 *m*/*z*; calcd for $[M+H]^+$: 326.1 *m*/*z*. IR (solid, cm^{-1}): 3244, 2716, 1738, 1607, 1194, 1121. UV/vis ε_{max} (223 nm): 27 500 M^{-1} cm^{-1}.

*fac-[Re^I(CO)$_3$(N,N,N-**3**)], **4**.* Ligand **3** (4.9 × 10^{-5} mol) was suspended in 2 mL H_2O and dissolved by adding 1 M $NaHCO_3$ until pH ∼7.5 was achieved. The pH was adjusted to 6.5−7 with 0.1 M HCl, and a 0.1 M solution of *fac*-$[Re^I(OH_2)_3(CO)_3](SO_3CF_3)$ (0.5 mL, 5 × 10^{-5} mol) was added. The solution was stirred at 70 °C for 6.5 h while maintaining pH 6.5−7 by addition of 1 M $NaHCO_3$ or 0.1 M HCl as needed. The reaction was then cooled, filtered, and purified by preparatory RP-HPLC using a gradient method (prep-HPLC method 2) with the following conditions: 10 mL/min; 0−3 min 100% A, 3−10 min 75% A/25% B, 10−32 min linear gradient to 100% B, 32−40 min 100% B, 40−45 min equilibrate in 100% A; UV at 220 nm. Product peak t_R: 26.6 min. Purified portions were combined and concentrated to dryness under vacuum to yield 19 mg (66%) of the desired product as a grayish-brown powder. X-ray quality crystals were obtained by vapor diffusion of ethyl acetate into a solution of **4** dissolved in EtOH. Anal. Calcd for $C_{20}H_{14}N_3O_7Re \cdot H_2O$: C, 39.22; H, 2.63; N, 6.86. Found: C, 39.77; H, 2.40; N, 6.47. ^{1}H NMR [δ (ppm), 300 MHz, CD_3OD]: 9.33 (d, $C_{Py}H$, 2 H), 8.48 (dd, $C_{Py}H$, 2 H), 7.71 (d, $C_{Py}H$, 2 H), 5.03 (d, *J* = 18.0 Hz, Py-CH_{2A}-N, 2 H), 4.96 (d, *J* = 17.7 Hz, Py-CH_{2B}-N, 2 H), 4.64 (d, N-CH_2-C, 2 H), 3.41 (dd, CC*H*, 1 H). ^{13}C NMR [δ (ppm), 75 MHz, CD_3OD]: 165.3 (COO), 165.1 (Ar-C), 154.1 (Ar-C), 142.2 (Ar-C), 130.7 (Ar-C), 124.7 (Ar-C), 80.8 (N-CH_2), 77.3 (N-CH_2), 69.1 (CH_2-C≡CH), 58.9 (C≡CH). MS (+ESI): 596.1 *m*/*z*; calcd for $[M]^+$: 596.1 *m*/*z*. IR (solid, cm^{-1}): 2033, 1937, 1678, 1183, 1124. UV/vis ε_{max} (213 nm): 19 600 M^{-1} cm^{-1}.

Cys-NAPamide Analogue Synthesis, Functionalization, and Complexation Reactions. *Ac-Cys-Nle-Asp-His-$_D$-Phe-Arg-Trp-Gly-Lys-NH$_2$, **5**.* The starting peptide **5** (also abbreviated as Cys-NAPamide) was synthesized on an automated CS Bio CS336 peptide synthesizer (CS Bio Company, Inc., Menlo Park, CA) using standard solid-phase techniques with Fmoc-protected amino acids. Briefly, Rink Amide LS resin (220 mg, 0.2 mmol, 0.44 mmol/g loading capacity) was presuspended and swollen in *N*,*N*-dimethylformamide (DMF) for 30 min. Fmoc groups on the resin beads were deprotected with 20% piperidine in DMF. For every step, each Fmoc-protected amino acid (1 mmol) was activated in a solution containing 1 mmol HOBt and 1 M diisopropylcarbodiimide in DMF. After deprotection of the Fmoc protection group of the last amino acid residue, the *N*-terminal residue was acetylated by acetic anhydride with HOBt/diisopropylethylamine. The resultant peptide was cleaved and deprotected by a 3 h incubation in a mixture of TFA/triisopropylsilane/1,2-ethanedithiol/H_2O (94:2:2:2). The crude peptide was filtered, and then precipitated with ice-cold anhydrous diethyl ether. The resulting peptide pellet was washed four times with ice-cold anhydrous diethyl ether, dried under a flow of N_2, and

dx.doi.org/10.1021/bc5000115 | *Bioconjugate Chem.* 2014, 25, 579−592

dissolved in a 1 mM dithiothreitol solution. The crude peptide was purified by semipreparative RP-HPLC with solvents A (0.1% TFA in H_2O) and C (0.1% TFA in MeCN) using a linear gradient from 95% A/5% C to 35% A/65% C over 45 min at a flow rate of 4 mL/min. Purified fractions were collected and lyophilized to yield the desired peptide, **5**, in 83% yield and >95% purity by analytical RP-HPLC using HPLC method 3 (gradient system with solvents A and C; 1 mL/min flow rate; 0−3 min 95% A/5% C, 3−33 min linear gradient to 35% A/65% C, 33−36 min linear gradient to 15% A/85% C, hold 15% A/85% C from 36 to 39 min, return to 95% A/5% C at 39 min and equilibrate in 95% A/5% C; UV at 238 nm). MS (+ESI): 602.1 *m/z*, 1202.5 *m/z*; calcd for $[M+2H]^{2+}$: 601.8 *m/z*; calcd for $[M+H]^{+}$: 1202.6 *m/z*.

*Ac-S-(3-Azidopropyl)-acetamido-Cys-Nle-Asp-His-D-Phe-Arg-Trp-Gly-Lys-NH$_2$, **6**.* Peptide **5** (2.1 mg, 1.36×10^{-6} mol) was dissolved in 1.2 mL 0.1 M pH 7.4 PBS and mixed with 1.2 mL TCEP gel (tris-2-carboxyethyl phosphine, Pierce) in 0.1 M pH 7.4 PBS at room temperature for 1.75 h. The gel was removed by filtration, and the filtrate was immediately frozen and lyophilized overnight. N_2-sparged water (1 mL), N_2-sparged MeCN (0.35 mL), and 2-bromo-*N*-(3-azidopropyl)-acetamide (0.45 mg, 2.0×10^{-6} mol) were added to the reduced peptide, and the solution was stirred at room temperature for 12 h. The reaction mixture was subsequently concentrated by rotary evaporation and purified by RP-HPLC using HPLC method 3. MeCN was removed from the purified product fractions under vacuum, and the resulting purified solution was frozen and lyophilized overnight to yield 1.6 mg (70%) of **6**. MS (+ESI): 672.0 *m/z*, 1343.1 *m/z*; calcd for $[M+2H]^{2+}$: 671.8 *m/z*; calcd for $[M+H]^{+}$: 1342.7 *m/z*. IR (lyophilized solid, cm^{-1}): 3271, 3206, 2103, 1659, 1642, 1536, 1427, 1181, 1130.

Ellman's Test for Thiol Content. Peptide **6** was analyzed by a 5,5′-dithio-*bis*-(2-nitrobenzoic acid) (DTNB, Ellman's reagent) assay according to instructions from Pierce, with slight modifications. Briefly, triplicate solutions of **6** at 3.5×10^{-4} to 4×10^{-4} M in 50 μL H_2O were combined with 500 μL Ellman's buffer (0.1 M pH 8 sodium phosphate with 1 mM EDTA) and 10 μL DTNB dissolved at 4 mg/mL in Ellman's buffer. The solutions were vortexed and allowed to sit at room temperature for 15 min, and the UV absorbance of the solutions at 412 nm was determined. The amount of free thiol remaining in the peptide solutions was quantified by comparing the absorbance values at 412 nm to a standard curve generated by performing the assay with freshly prepared solutions of L-cysteine at known concentrations.

*CuAAC Conjugate of Peptide **6** and Ligand **1**, **7**.* Peptide **6** (300 μg, 1.78×10^{-7} mol) in 70 μL H_2O, **1** (2.29×10^{-7} mol) in 10.9 μL MeOH, sodium ascorbate (6.4×10^{-7} mol), copper(II) acetate ($Cu(OAc)_2$, 3.2×10^{-7} mol), and 100 μL of 0.1 M pH 7.4 PBS were combined, and the reaction was stirred under argon at room temperature for 2 h. A solution of 0.1 M EDTA (100 μL, 1×10^{-5} mol) was added and the solution was stirred at room temperature overnight. The reaction mixture was then acidified with 10% TFA in H_2O and purified by RP-HPLC using a gradient method (HPLC method 4: 1 mL/min flow rate; 0−3 min 95% A/5% B, 3−33 min linear gradient to 35% A/65% B, 33−36 min linear gradient to 1% A/99% B, hold 1% A/99% B from 36 to 39 min, return to 95% A/5% B at 39 min and equilibrate in 95% A/5% B; UV at 238 nm). MeOH was removed from the purified product fractions under vacuum, and the resulting purified solution was frozen and lyophilized overnight to yield 200 μg (51%) of **7**. MS (+ESI): 790.7 *m/z*, 527.6 *m/z*, 821.2 *m/z*; calcd for $[M+2H]^{2+}$: 790.4 *m/z*; calcd for $[M+3H]^{3+}$: 527.3 *m/z*; calcd for $[M+2H+Cu]^{2+}$: 821.9 *m/z*. This reaction was repeated several times to obtain additional product for reactions below.

*CuAAC Conjugate of Peptide **6** and Ligand **3**, **8**.* Peptide **6** (420 μg, 2.49×10^{-7} mol) in 70 μL 0.1 M pH 7.4 PBS, **3** (3×10^{-7} mol) in 32.5 μL H_2O, sodium ascorbate (9×10^{-7} mol), $Cu(OAc)_2$ (4.5×10^{-7} mol), and 20 μL of 0.1 M pH 7.4 PBS were combined, and the reaction was stirred under argon at room temperature for 3 h. Sodium sulfide (3 mg, 1.25×10^{-5} mol) was added and the solution was stirred at room temperature for 2.75 h. The reaction mixture was then acidified with 10% TFA in H_2O, centrifuged, and the supernatant was purified by RP-HPLC with HPLC method 4. Methanol was removed from the purified product fractions under vacuum, and the resulting purified solution was frozen and lyophilized overnight to yield 350 μg (61%) of **8**. MS (+ESI): 834.7 *m/z*, 557.0 *m/z*, 866.2 *m/z*, 1667.6 *m/z*; calcd for $[M+2H]^{2+}$: 834.4 *m/z*; calcd for $[M+3H]^{3+}$: 556.6 *m/z*; calcd for $[M+2H+Cu]^{2+}$: 865.8 *m/z*; calcd for $[M+H]^{+}$: 1667.8 *m/z*. This reaction was repeated several times to obtain additional product for reactions below.

*Click, then Chelate Route for Generating Conjugate of Peptide **7** and fac-[Re^{I}(CO)$_3$]$^{+}$, **9**.* Peptide 7 (200 μg, 9.5×10^{-8} mol) in 300 μL 0.1 M pH 7.4 PBS and 1 μL 0.1 M *fac*-$[Re^{I}(OH_2)_3(CO)_3](SO_3CF_3)$ (1×10^{-7} mol) were combined in a vial and stirred under argon at 60 °C for 1.75 h. Following the reaction, the solution was acidified with 0.1% TFA and purified by RP-HPLC with solvents A and B using a gradient method (HPLC method 5: 1 mL/min flow rate; 0−15 min 62% A/38% B, 15−40 min linear gradient to 100% B, 40−45 min hold 100% B, return to 62% A/38% B at 34 min and equilibrate; UV at 220 nm). Methanol was removed from the purified product fractions under vacuum, and the resulting purified solution was frozen and lyophilized overnight to yield 200 μg (9.3×10^{-8} mol, 98%) of **9**. MS (+ESI): 617.7 *m/z*, 925.7 *m/z*; calcd for $[M+2H]^{3+}$: 617.2 *m/z*; calcd for $[M+H]^{2+}$: 925.4 *m/z*.

*Chelate, then Click Route for Generating CuAAC Conjugate of Peptide **6** and Complex **2**, **9′**.* Peptide **6** (300 μg, 1.78×10^{-7} mol) in 25 μL H_2O and **2** (1.81×10^{-7} mol) in MeOH were combined, and the MeOH was removed by rotary evaporation. Sodium ascorbate (3.8×10^{-7} mol) in 3.55 μL 0.1 M pH 6 PBS and $Cu(OAc)_2$ (1.9×10^{-7} mol) in 3.33 μL 0.1 M pH 6 PBS were added, and the reaction vial was purged with N_2 for 2 min. The reaction was stirred at room temperature overnight and then purified by RP-HPLC with HPLC method 5. Methanol was removed from the purified product fractions under vacuum, and the resulting purified solution was frozen and lyophilized overnight to yield 200 μg (8.3×10^{-8} mol, 47%) of **9′**. MS (+ESI): 617.7 *m/z*, 925.5 *m/z*; calcd for $[M+2H]^{3+}$: 617.2 *m/z*; calcd for $[M+H]^{2+}$: 925.4 *m/z*.

*Click, then Chelate Route for Generating Conjugate of Peptide **8** and fac-[Re^{I}(CO)$_3$]$^{+}$, **10**.* Peptide **8** (300 μg, 1.37×10^{-7} mol) in 200 μL H_2O, 100 μL 0.1 M pH 7.4 PBS, and 1.5 μL 0.1 M *fac*-$[Re^{I}(OH_2)_3(CO)_3](SO_3CF_3)$ (1.5×10^{-7} mol) were combined in a vial and stirred under argon at 60 °C for 2.25 h. Following the reaction, the solution was acidified with 0.1% TFA and purified by RP-HPLC with HPLC method 5. Methanol was removed from the purified product fractions under vacuum, and the resulting purified solution was frozen and lyophilized overnight to yield 200 μg (8.8×10^{-8} mol,

dx.doi.org/10.1021/bc5000115 | *Bioconjugate Chem.* 2014, 25, 579−592

64%) of **10**. MS (+ESI): 968.7 m/z; calcd for $[M+H]^{2+}$: 968.9 m/z.

*Chelate, then Click Route for Generating CuAAC Conjugate of Peptide **6** and Complex **4**, **10′***. Peptide **6** (200 μg, 1.19×10^{-7} mol), **4** (1.6×10^{-7} mol), sodium ascorbate (2.55×10^{-7} mol), and $Cu(OAc)_2$ (1.28×10^{-7} mol) were dissolved in 100 μL of 0.1 M pH 6 PBS; the reaction vial was purged with N_2 for 2 min and then stirred at room temperature for a total of 48 h with the addition of more sodium ascorbate (2.55×10^{-7} mol) and $Cu(OAc)_2$ (5.8×10^{-8} M) after the first 24 h. After a total reaction time of 48 h, EDTA (2×10^{-6} mol) was added and the reaction was stirred for 1 h. The reaction was then acidified with TFA (2.5 μL), and the solution was centrifuged to pellet the resulting precipitate. The supernatant was collected and purified by RP-HPLC with HPLC method 5. Methanol was removed from the purified product fractions under vacuum, and the resulting purified solution was frozen and lyophilized overnight to yield 200 μg (8.8×10^{-8} mol, 70%) of **10′**. MS (-ESI): 1936.3 m/z; calcd for $[M-H]^-$: 1936.7 m/z.

^{99m}Tc Reactions with Small Molecules and Peptides. *General Procedures for ^{99m}Tc Reactions with Small Molecule Ligands.* Solutions of **1** or **3** in 10 mM pH 7.2 PBS (400−450 μL) were sealed in 5 mL labeling vials and the vials were purged with N_2 for 5−10 min. Solutions of *fac*-$[^{99m}Tc^{I}(OH_2)_3(CO)_3]^+$ (50−100 μL, 0.98−1.37 mCi) were added to bring the final ligand concentrations to 1×10^{-4} to 1×10^{-6} M in final volumes of 500 μL, and the vials were heated at 70 °C for 30−60 min. The vials were cooled prior to analysis and purification by radio-HPLC using HPLC method 1.

General Procedures for ^{99m}Tc Reactions with Peptides. Click, then chelate route: Solutions of peptides **7** or **8** (2.5×10^{-8} mol) dissolved in 400 μL 10 mM pH 7.4 PBS were sealed in 5 mL labeling vials and purged with N_2 for 5−10 min. 100 uL of *fac*-$[^{99m}Tc(OH_2)_3(CO)_3]^+$ (0.76−0.81 mCi) was added to yield final peptide concentrations of 5×10^{-5} M. The reactions were heated at 70 °C for a total of 1 h with monitoring by RP-HPLC using HPLC method 1 or HPLC method 6 (solvents A and B; 1 mL/min flow rate; 0−8 min 62% A/38% B, 8−26 min linear gradient to 100% B, 26−30 min hold 100% B, return to 62% A/38% B after 30 min and equilibrate; UV at 220, 238, or 254 nm). Peptides were purified by HPLC method 1 or HPLC method 6. *Chelate, then click* route: Crude reaction mixtures of either **2a** or **4a** (200 μL, 0.34−0.60 mCi) containing ligands **1** or **3** at 5.25×10^{-5} M were added to a solution containing peptide **6** (2.6×10^{-8} mol) and sodium ascorbate (2×10^{-6} mol) in 10 mM pH 7.4 PBS (275 μL) in 5 mL labeling vials. After the vials were sealed and purged with N_2 for 5 min, $Cu(OAc)_2$ (1×10^{-6} mol) was added to give a final volume of 500 μL with peptide **6** at 5.2×10^{-5} M, ligands **1** or **3** at 2.1×10^{-5} M, sodium ascorbate at 4×10^{-3} M, and $Cu(OAc)_2$ at 2×10^{-3} M. The vials were then heated with stirring at 50 °C for a total of 1 h with periodic monitoring by radio-HPLC using HPLC method 6. Peptides were purified by either HPLC method 1 or HPLC method 6.

Stability Analysis. Solutions of HPLC-purified **4a**, **9a**, **9a′**, **10a**, or **10a′** (200 μL, MeOH removed under a stream of N_2 following isolation) were combined with solutions containing L-histidine or L-cysteine at 2×10^{-3} M in 10 mM pH 7.4 PBS (200 μL) in 5 mL labeling vials. Vials were sealed, purged with N_2 for 5 min, and incubated at 37 °C for a total of 18 h (**9a**, **9a′**, **10a**, and **10a′**) or 24 h (**4a**) with periodic analysis by radio-HPLC using HPLC methods 1 or 6. Serum stability of **4a** was determined by incubating solutions of HPLC-purified **4a** (200 μL) in mouse serum (200 μL, clarified by centrifugation) in 5 mL labeling vials. Vials were sealed, purged with N_2 for 5 min, and incubated at 37 °C for a total of 24 h. At periodic time points, aliquots were removed, counted, and added to an equal volume of ice-cold ethanol to precipitate proteins from the solution. This mixture was centrifuged and the supernatants were counted and analyzed by radio-HPLC using HPLC method 1. Serum stability of the peptides was analyzed by incubating solutions of HPLC-purified **9a**, **9a′**, **10a**, or **10a′** (100 μCi) in 50 μL of 10 mM pH 7.4 PBS with mouse serum (500 μL) at 37 °C for a total of 6 h. At periodic time points, the solutions were filtered through a centrifugal filter (10 K; Millipore Corp.) and the filtrate was analyzed by radio-HPLC using HPLC method 2.

Log P analysis. Equal volumes of 10 mM pH 7.4 PBS and 1-octanol (500 μL each) were vortexed (30 s) in centrifuge tubes and allowed to separate (2 min). HPLC-purified solutions of **2a**, **4a**, **9a′**, or **10a′** (0.1 μCi in 2−15 μL, MeOH removed under a stream of N_2 following isolation) were added to triplicate sets of tubes after an equal volume of the aqueous phase was removed, and the tubes were vortexed (1 min) and centrifuged (2000 × g, 5 min). Aliquots (50 μL) from each layer were removed and counted to determine the ratio of radioactivity present in the octanol layer compared to the aqueous layer.

In Vitro and In Vivo Biological Evaluations. *Cell Culture and Animal Model.* Cell growth and tumor implantation procedures were performed as previously described.[41] Briefly, B16F10 murine melanoma cells were cultured in Dulbecco's modified Eagle's high-glucose medium (GIBCO, Carlsbad, CA) and supplemented with 10% fetal bovine serum (FBS) and 1% penicillin−streptomycin in a humidified incubator containing 5% CO_2 at 37 °C. A 70−80% confluent monolayer was detached with 0.25% trypsin−EDTA and dissociated into a single-cell suspension for further cell culture and assays. All animal studies were carried out in compliance with federal and local institutional rules for the conduct of animal experimentation. Approximately 1×10^6 cultured B16F10 cells were suspended in 100 μL of PBS and subcutaneously implanted in the right shoulders of C57BL/6 mice. Tumors were grown to a size of 0.5−1 cm in diameter (1−2 weeks) prior to biodistribution studies.

In Vitro IC_{50} Cell Binding Analysis. The MC1R binding affinity of **5**, **6**, **9′**, and **10′** in B16F10 cells was performed as previously described.[41] Briefly, B16F10 cells (5×10^5) suspended in Dulbecco's Modified Eagle's Medium (DMEM) containing 25 mM *N*-(2-hydroxyethyl)piperazine-*N′*-(2-ethanesulfonic acid), 0.2% bovine serum albumin, and 0.3 mM 1,10-phenanthroline were seeded at a density of 0.3 million per well in 96-well plates and allowed to attach overnight. The cells were then incubated at 37 °C for 2 h with ^{125}I-(Tyr^2)-NDP (20 000 counts per minute) and **5**, **6**, **9′**, or **10′** (peptide concentration varying from 10^{-11} to 10^{-5} M). Cells were washed three times with ice-cold 10 mM pH 7.4 PBS and lysed in 1 mL of 1.0 M NaOH containing 0.1% sodium dodecyl sulfate. The radioactivity of the lysed cells was measured by a γ-counter (Perkin-Elmer model 1470). The experiment was performed in quadruplicate wells. The IC_{50} values (the concentration of competitor required to inhibit 50% of the radioligand binding) of the peptides were calculated by using Origin 8.0 (MicroCal).

dx.doi.org/10.1021/bc5000115 | *Bioconjugate Chem.* 2014, 25, 579−592

In Vitro B16F10 Melanoma Cell Uptake Assays. Cell uptake studies of **9a′** and **10a′** were performed as previously described.[41] Briefly, B16F10 cells (3×10^5) were seeded in 12-well tissue culture plates and incubated at 37 °C overnight. The cells were washed with 10 mM pH 7.4 PBS and then incubated with **9a′** or **10a′** (1 μCi per well, in DMEM) with or without NDP (3 μM/well) at 37 °C for 0.5, 1, and 2 h. The cells were then washed 3 times with 10 mM pH 7.4 PBS and lysed in 1 mL of 1.0 M NaOH containing 0.1% sodium dodecyl sulfate and transferred to γ-counter tubes. Radioactivity was measured by a γ-counter (Perkin-Elmer model 1470). Cell uptake was expressed as the percentage of added radioactivity. Experiments were performed twice with quadruplicate wells.

In Vivo B16F10 Melanoma Xenograft Mouse Biodistribution Analysis. For biodistribution studies, female C57BL/6 mice bearing B16F10 xenografts (n = 4 per group) were injected via the tail vein with approximately 100 μCi of **9a′** or **10a′** and were euthanized at 1 and 2 h post injection (p.i.). Tumor and normal tissues of interest were removed and weighed, and their radioactivity was measured using a γ-counter. Radioactivity uptake was expressed as a percentage of the injected radioactive dose per gram of tissue (% ID/g).

Statistical Methods. Statistical analysis was performed using the Student's t test for unpaired data. A 95% confidence level was chosen to determine the significance between groups, with $P < 0.05$ being designated as significantly different.

■ ASSOCIATED CONTENT

Supporting Information

Radiolabeling yields for **4a**. In vitro stability of **4a**, **9a′**, and **10a′**. Log P analysis of **2a**, **4a**, **9a′**, and **10a′**. RP-HPLC chromatograms of all peptides. X-ray crystallography experimental procedures and tables with crystal data, structure refinement, bond lengths, bond angles, and hydrogen bonds for **4** (CCDC deposition number: 975046). This material is available free of charge via the Internet at http://pubs.acs.org.

■ AUTHOR INFORMATION

Corresponding Authors

*E-mail: zcheng@stanford.edu. Phone: (650) 723-7866. Fax: (650) 736-7925.

*E-mail: bennyp@wsu.edu. Phone: (509) 335-3858. Fax: (509) 335-8867.

Author Contributions

Benjamin B. Kasten and Xiaowei Ma contributed equally to this work.

Notes

The authors declare no competing financial interest.

■ ACKNOWLEDGMENTS

The authors wish to thank Mary Dyszlewski of Covidien, Inc. for the Isolink kits. This research was funded in part by the NIH Biotechnology Training Program at Washington State University (T32 GM008336) and the Office of Science (BER), U.S. Department of Energy (DE-SC0008397).

■ ABBREVIATIONS

cpm, counts per minute; CuAAC, copper(I)-catalyzed azide–alkyne cycloaddition; $Cu(OAc)_2$, copper(II) acetate; Cys-NAPamide, Ac-Cys-Nle-Asp-His-D-Phe-Arg-Trp-Gly-Lys-NH_2; DMF, *N*,*N*-dimethylformamide; DMEM, Dulbecco's Modified Eagle's Medium; DPA, 2,2′-dipicolylamine; DTNB, 5,5′-dithio-*bis*-(2-nitrobenzoic acid); EDTA, ethylenediaminetetraacetic acid; ESI-MS, electrospray ionization mass spectrometry; EtOH, ethanol; Fmoc, 9-fluorenylmethoxycarbonyl; HOBt, hydroxybenzotriazole; HPLC, high performance liquid chromatography; ^{125}I-(Tyr^2)-NDP, ^{125}I-(Tyr^2)-[Nle^4,D-Phe^7]-α-MSH; % ID/g, percent injected dose per gram of tissue; IR, infrared; MC1R, melanocortin 1 receptor; MeCN, acetonitrile; MeOH, methanol; α-MSH, alpha-melanocyte stimulating hormone; NAPamide, Ac-Nle-Asp-His-D-Phe-Arg-Trp-Gly-Lys-NH_2; NMR, nuclear magnetic resonance; PBS, phosphate buffered saline; p.i., post injection; RP-HPLC, reversed-phase HPLC; SPECT, single photon emission computed tomography; TCEP, tris-2-carboxyethyl phosphine; TFA, trifluoroacetic acid

■ REFERENCES

(1) Rostovtsev, V. V., Green, L. G., Fokin, V. V., and Sharpless, K. B. (2002) A stepwise Huisgen cycloaddition process: copper(I)-catalyzed regioselective "ligation" of azides and terminal alkynes. *Angew. Chem., Int. Ed. 41*, 2596–2599.

(2) Tornøe, C. W., Christensen, C., and Meldal, M. (2002) Peptidotriazoles on solid phase: [1,2,3]-triazoles by regiospecific copper(I)-catalyzed 1,3-dipolar cycloadditions of terminal alkynes to azides. *J. Org. Chem. 67*, 3057–3064.

(3) Hein, C., Liu, X.-M., and Wang, D. (2008) Click chemistry, a powerful tool for pharmaceutical sciences. *Pharm. Res. 25*, 2216–2230.

(4) Tron, G. C., Pirali, T., Billington, R. A., Canonico, P. L., Sorba, G., and Genazzani, A. A. (2008) Click chemistry reactions in medicinal chemistry: Applications of the 1,3-dipolar cycloaddition between azides and alkynes. *Med. Res. Rev. 28*, 278–308.

(5) Amblard, F., Cho, J. H., and Schinazi, R. F. (2009) Cu(I)-catalyzed Huisgen azide-alkyne 1,3-dipolar cycloaddition reaction in nucleoside, nucleotide, and oligonucleotide chemistry. *Chem. Rev. 109*, 4207–4220.

(6) Kiick, K. L., Saxon, E., Tirrell, D. A., and Bertozzi, C. R. (2002) Incorporation of azides into recombinant proteins for chemoselective modification by the Staudinger ligation. *Proc. Natl. Acad. Sci. U. S. A. 99*, 19–24.

(7) Chin, J. W., Santoro, S. W., Martin, A. B., King, D. S., Wang, L., and Schultz, P. G. (2002) Addition of *p*-azido-L-phenylalanine to the genetic code of *Escherichia coli*. *J. Am. Chem. Soc. 124*, 9026–9027.

(8) Nguyen, D. P., Lusic, H., Neumann, H., Kapadnis, P. B., Deiters, A., and Chin, J. W. (2009) Genetic encoding and labeling of aliphatic azides and alkynes in recombinant proteins via a pyrrolysyl-tRNA Synthetase/tRNACUA pair and click chemistry. *J. Am. Chem. Soc. 131*, 8720–8721.

(9) Mamat, C., Ramenda, T., and Wuest, F. R. (2009) Recent applications of click chemistry for the synthesis of radiotracers for molecular imaging. *Mini-Rev. Org. Chem. 6*, 21–34.

(10) Zeng, D., Zeglis, B. M., Lewis, J. S., and Anderson, C. J. (2013) The growing impact of bioorthogonal click chemistry on the development of radiopharmaceuticals. *J. Nucl. Med. 54*, 829–832.

(11) Waibel, R., Alberto, R., Willuda, J., Finnern, R., Schibli, R., Stichelberger, A., Egli, A., Abram, U., Mach, J.-P., Plückthun, A., and Schubiger, P. A. (1999) Stable one-step technetium-99m labeling of His-tagged recombinant proteins with a novel Tc(I)-carbonyl complex. *Nat. Biotechnol. 17*, 897–901.

(12) Egli, A., Alberto, R., Tannahill, L., Schibli, R., Abram, U., Schaffland, A., Waibel, R., Tourwe, D., Jeannin, L., Iterbeke, K., and Schubiger, P. A. (1999) Organometallic ^{99m}Tc-aquaion labels peptide to an unprecedented high specific activity. *J. Nucl. Med. 40*, 1913–1917.

(13) Alberto, R., Schibli, R., Egli, A., Schubiger, A. P., Abram, U., and Kaden, T. A. (1998) A novel organometallic aqua complex of technetium for the labeling of biomolecules: synthesis of $[^{99m}Tc(OH_2)_3(CO)_3]^+$ from $[^{99m}TcO_4]^-$ in aqueous solution and its reaction with a bifunctional ligand. *J. Am. Chem. Soc. 120*, 7987–7988.

(14) Alberto, R., Kyong Pak, J., van Staveren, D., Mundwiler, S., and Benny, P. (2004) Mono-, bi-, or tridentate ligands? The labeling of peptides with ^{99m}Tc-carbonyls. *Pept. Sci. 76*, 324−333.
(15) Ganguly, T., Kasten, B. B., Hayes, T. R., and Benny, P. D. (2012) Recent advances in Re/Tc radiopharmaceutical design utilizing orthogonal and metal template based click reactions, in *Advances in Chemistry Research* (Taylor, J. C., Ed.) pp 93−141, Nova Science Publishers, Inc., New York.
(16) Mindt, T. L., Struthers, H., Brans, L., Anguelov, T., Schweinsberg, C., Maes, V., Tourwé, D., and Schibli, R. (2006) "Click to chelate": synthesis and installation of metal chelates into biomolecules in a single step. *J. Am. Chem. Soc. 128*, 15096−15097.
(17) Kluba, C., and Mindt, T. (2013) Click-to-chelate: development of technetium and rhenium-tricarbonyl labeled radiopharmaceuticals. *Molecules 18*, 3206−3226.
(18) Schibli, R., La Bella, R., Alberto, R., Garcia-Garayoa, E., Ortner, K., Abram, U., and Schubiger, P. A. (2000) Influence of the denticity of ligand systems on the in vitro and in vivo behavior of ^{99m}Tc(I)-tricarbonyl complexes: a hint for the future functionalization of biomolecules. *Bioconjugate Chem. 11*, 345−351.
(19) Banerjee, S. R., Schaffer, P., Babich, J. W., Valliant, J. F., and Zubieta, J. (2005) Design and synthesis of site directed maleimide bifunctional chelators for technetium and rhenium. *Dalton Trans.*, 3886−3897.
(20) Liu, G., Dou, S., He, J., Vanderheyden, J.-L., Rusckowski, M., and Hnatowich, D. J. (2004) Preparation and properties of ^{99m}Tc-$(CO)_3^+$-labeled *N,N*-bis(2-pyridylmethyl)-4-aminobutyric acid. *Bioconjugate Chem. 15*, 1441−1446.
(21) Maresca, K. P., Hillier, S. M., Femia, F. J., Zimmerman, C. N., Levadala, M. K., Banerjee, S. R., Hicks, J., Sundararajan, C., Valliant, J., Zubieta, J., Eckelman, W. C., Joyal, J. L., and Babich, J. W. (2009) Comprehensive radiolabeling, stability, and tissue distribution studies of technetium-99m single amino acid chelates (SAAC). *Bioconjugate Chem. 20*, 1625−1633.
(22) Raposinho, P. D., Correia, J. D. G., Alves, S., Botelho, M. F., Santos, A. C., and Santos, I. (2008) A ^{99m}Tc$(CO)_3$-labeled pyrazolyl-α-melanocyte-stimulating hormone analog conjugate for melanoma targeting. *Nucl. Med. Biol. 35*, 91−99.
(23) Maresca, K. P., Marquis, J. C., Hillier, S. M., Lu, G., Femia, F. J., Zimmerman, C. N., Eckelman, W. C., Joyal, J. L., and Babich, J. W. (2010) Novel polar single amino acid chelates for technetium-99m tricarbonyl-based radiopharmaceuticals with enhanced renal clearance: application to octreotide. *Bioconjugate Chem. 21*, 1032−1042.
(24) Jemal, A., Siegel, R., Ward, E., Hao, Y., Xu, J., Murray, T., and Thun, M. J. (2008) Cancer statistics, 2008. *CA: Cancer J. Clin. 58*, 71−96.
(25) Anderson, C. M.; Buzaid, A. C.; Legha, S. S. Systemic treatments for advanced cutaneous melanoma. *Oncology (Williston Park)* 1995, *9*, 1149−1158; discussion 1163−1164, 1167−1168.
(26) Chen, J., Cheng, Z., Hoffman, T. J., Jurisson, S. S., and Quinn, T. P. (2000) Melanoma-targeting properties of ^{99m}Technetium-labeled cyclic α-melanocyte-stimulating hormone peptide analogues. *Cancer Res. 60*, 5649−5658.
(27) Marghoob, A. A., Slade, J., Salopek, T. G., Kopf, A. W., Bart, R. S., and Rigel, D. S. (1995) Basal cell and squamous cell carcinomas are important risk factors for cutaneous malignant melanoma. Screening implications. *Cancer 75*, 707−714.
(28) Quinn, T. P., Zhang, X., and Miao, Y. (2010) Targeted melanoma imaging and therapy with radiolabeled alpha-melanocyte stimulating hormone peptide analogues. *G. Ital. Dermatol. Venereol. 145*, 245−258.
(29) Ren, G., Pan, Y., and Cheng, Z. (2010) Molecular probes for malignant melanoma imaging. *Curr. Pharm. Biotechnol. 11*, 590−602.
(30) Correia, J. D. G., Paulo, A., Raposinho, P. D., and Santos, I. (2011) Radiometallated peptides for molecular imaging and targeted therapy. *Dalton Trans. 40*, 6144−6167.
(31) Flook, A. M., Yang, J., and Miao, Y. (2013) Evaluation of new Tc-99m-labeled Arg-X-Asp-conjugated alpha-melanocyte stimulating hormone peptides for melanoma imaging. *Mol. Pharmaceutics 10*, 3417−3424.
(32) Guo, H., Gallazzi, F., and Miao, Y. (2013) Design and evaluation of new Tc-99m-labeled lactam bridge-cyclized alpha-MSH peptides for melanoma imaging. *Mol. Pharmaceutics 10*, 1400−1408.
(33) Morais, M., Oliveira, B. L., Correia, J. D. G., Oliveira, M. C., Jiménez, M. A., Santos, I., and Raposinho, P. D. (2013) Influence of the bifunctional chelator on the pharmacokinetic properties of ^{99m}Tc-$(CO)_3$-labeled cyclic α-melanocyte stimulating hormone analog. *J. Med. Chem. 56*, 1961−1973.
(34) Morais, M., Raposinho, P. D., Oliveira, M. C., Correia, J. D. G., and Santos, I. (2012) Evaluation of novel ^{99m}Tc(I)-labeled homobivalent α-melanocyte-stimulating hormone analogs for melanocortin-1 receptor targeting. *J. Biol. Inorg. Chem. 17*, 491−505.
(35) Morais, M., Raposinho, P. D., Oliveira, M. C., Pantoja-Uceda, D., Jiménez, M. A., Santos, I., and Correia, J. D. G. (2012) NMR structural analysis of MC1R-targeted rhenium(I) metallopeptides and biological evaluation of ^{99m}Tc(I) congeners. *Organometallics 31*, 5929−5939.
(36) Siegrist, W., Solca, F., Stutz, S., Giuffrè, L., Carrel, S., Girard, J., and Eberle, A. N. (1989) Characterization of receptors for α-melanocyte-stimulating hormone on human melanoma cells. *Cancer Res. 49*, 6352−6358.
(37) Salazar-Onfray, F., Lopez, M., Lundqvist, A., Aguirre, A., Escobar, A., Serrano, A., Korenblit, C., Petersson, M., Chhajlani, V., Larsson, O., and Kiessling, R. (2002) Tissue distribution and differential expression of melanocortin 1 receptor, a malignant melanoma marker. *Br. J. Cancer 87*, 414−422.
(38) Lopez, M. N., Pereda, C., Ramirez, M., Mendoza-Naranjo, A., Serrano, A., Ferreira, A., Poblete, R., Kalergis, A. M., Kiessling, R., and Salazar-Onfray, F. (2007) Melanocortin 1 receptor is expressed by uveal malignant melanoma and can be considered a new target for diagnosis and immunotherapy. *Invest. Ophthalmol. Vis. Sci. 48*, 1219−1227.
(39) Cheng, Z., Xiong, Z., Subbarayan, M., Chen, X., and Gambhir, S. S. (2007) ^{64}Cu-labeled alpha-melanocyte-stimulating hormone analog for microPET imaging of melanocortin 1 receptor expression. *Bioconjugate Chem. 18*, 765−772.
(40) Raposinho, P., Xavier, C., Correia, J., Falcão, S., Gomes, P., and Santos, I. (2008) Melanoma targeting with α-melanocyte stimulating hormone analogs labeled with *fac*-[^{99m}Tc$(CO)_3]^+$: effect of cyclization on tumor-seeking properties. *J. Biol. Inorg. Chem. 13*, 449−459.
(41) Jiang, H., Kasten, B. B., Liu, H., Qi, S., Liu, Y., Tian, M., Barnes, C. L., Zhang, H., Cheng, Z., and Benny, P. D. (2012) Novel, cysteine-modified chelation strategy for the incorporation of $[M^I(CO)_3]^+$ (M = Re, ^{99m}Tc) in an α-MSH peptide. *Bioconjugate Chem. 23*, 2300−2312.
(42) Moura, C., Gano, L., Mendes, F., Raposinho, P. D., Abrantes, A. M., Botelho, M. F., Santos, I., and Paulo, A. (2012) ^{99m}Tc(I)/Re(I) tricarbonyl complexes for *in vivo* targeting of melanotic melanoma: Synthesis and biological evaluation. *Eur. J. Med. Chem. 50*, 350−360.
(43) He, H., Lipowska, M., Xu, X., Taylor, A. T., Carlone, M., and Marzilli, L. G. (2005) $Re(CO)_3$ complexes synthesized via an improved preparation of aqueous *fac*-$[Re(CO)_3(H_2O)_3]^+$ as an aid in assessing ^{99m}Tc imaging agents. Structural characterization and solution behavior of complexes with thioether-bearing amino acids as tridentate ligands. *Inorg. Chem. 44*, 5437−5446.
(44) Bigey, P., Frau, S., Loup, C., Claparols, C., Bernadou, J., and Meunier, B. (1996) Preparation and characterization by electrospray mass spectrometry of cationic metalloporphyrin DNA cleavers. *Bull. Soc. Chim. Fr. 133*, 679−689.
(45) Lam, C. F. C., Giddens, A. C., Chand, N., Webb, V. L., and Copp, B. R. (2012) Semi-synthesis of bioactive fluorescent analogues of the cytotoxic marine alkaloid discorhabdin C. *Tetrahedron 68*, 3187−3194.
(46) Huang, S., Clark, R. J., and Zhu, L. (2007) Highly sensitive fluorescent probes for zinc ion based on triazolyl-containing tetradentate coordination motifs. *Org. Lett. 9*, 4999−5002.
(47) Moore, A. L., Bucar, D.-K., MacGillivray, L. R., and Benny, P. D. (2010) "Click" labeling strategy for $M(CO)_3$ (M = Re, ^{99m}Tc)

prostate cancer targeted Flutamide agents. *Dalton Trans. 39*, 1926−1928.
(48) He, H., Morley, J. E., Twamley, B., Groeneman, R. H., Bučar, D.-K., MacGillivray, L. R., and Benny, P. D. (2009) Investigation of the coordination interactions of S-(pyridin-2-ylmethyl)-L-cysteine ligands with $M(CO)_3^+$ (M = Re, ^{99m}Tc). *Inorg. Chem. 48*, 10625−10634.
(49) Banerjee, S. R., Levadala, M. K., Lazarova, N., Wei, L., Valliant, J. F., Stephenson, K. A., Babich, J. W., Maresca, K. P., and Zubieta, J. (2002) Bifunctional single amino acid chelates for labeling of biomolecules with the $\{Tc(CO)_3\}^+$ and $\{Re(CO)_3\}^+$ cores. Crystal and molecular structures of $[ReBr(CO)_3(H_2NCH_2C_5H_4N)]$, $[Re(CO)_3\{(C_5H_4NCH_2)_2NH\}]Br$, $[Re(CO)_3\{(C_5H_4NCH_2)_2NCH_2CO_2H\}]Br$, $[Re(CO)_3\{X(Y)NCH_2CO_2CH_2CH_3\}]Br$ (X = Y = 2-pyridylmethyl; X = 2-pyridylmethyl, Y = 2-(1-methylimidazolyl)methyl; X = Y = 2-(1-methylimidazolyl)methyl), $[ReBr(CO)_3\{(C_5H_4NCH_2)NH(CH_2C_4H_3S)\}]$, and $[Re(CO)_3\{(C_5H_4NCH_2)N(CH_2C_4H_3S)(CH_2CO_2)\}]$. *Inorg. Chem. 41*, 6417−6425.
(50) Ganguly, T., Kasten, B. B., Bučar, D.-K., MacGillivray, L. R., Berkman, C. E., and Benny, P. D. (2011) The hydrazide/hydrazone click reaction as a biomolecule labeling strategy for $M(CO)_3$ (M = Re, ^{99m}Tc) radiopharmaceuticals. *Chem. Commun. (Cambridge, U. K.) 47*, 12846−12848.
(51) Benoist, E., Coulais, Y., Almant, M., Kovensky, J., Moreau, V., Lesur, D., Artigau, M., Picard, C., Galaup, C., and Gouin, S. G. (2011) A Click procedure with heterogeneous copper to tether technetium-99m chelating agents and rhenium complexes. Evaluation of the chelating properties and biodistribution of the new radiolabelled glucose conjugates. *Carbohydr. Res. 346*, 26−34.
(52) Cheng, Z., Zhang, L., Graves, E., Xiong, Z., Dandekar, M., Chen, X., and Gambhir, S. S. (2007) Small-animal PET of melanocortin 1 receptor expression using a ^{18}F-labeled α-melanocyte-stimulating hormone analog. *J. Nucl. Med. 48*, 987−994.
(53) Froidevaux, S., Calame-Christe, M., Tanner, H., and Eberle, A. N. (2005) Melanoma targeting with DOTA-α-melanocyte-stimulating hormone analogs: Structural parameters affecting tumor uptake and kidney uptake. *J. Nucl. Med. 46*, 887−895.
(54) Banerjee, S. R., Babich, J. W., and Zubieta, J. (2005) Site directed maleimide bifunctional chelators for the $M(CO)_3^+$ core (M = ^{99m}Tc, Re). *Chem. Commun. (Cambridge, U. K.)*, 1784−1786.
(55) Ahlgren, S., Wållberg, H., Tran, T. A., Widström, C., Hjertman, M., Abrahmsén, L., Berndorff, D., Dinkelborg, L. M., Cyr, J. E., Feldwisch, J., Orlova, A., and Tolmachev, V. (2009) Targeting of HER2-expressing tumors with a site-specifically ^{99m}Tc-labeled recombinant affibody molecule, $Z_{HER2:2395}$, with C-terminally engineered cysteine. *J. Nucl. Med. 50*, 781−789.
(56) Wang, Q., Chan, T. R., Hilgraf, R., Fokin, V. V., Sharpless, K. B., and Finn, M. G. (2003) Bioconjugation by copper(I)-catalyzed azide-alkyne [3 + 2] cycloaddition. *J. Am. Chem. Soc. 125*, 3192−3193.
(57) Hirva, P., Nielsen, A., Bond, A. D., and McKenzie, C. J. (2010) Potential cross-linking transition metal complexes (M = Ni, Cu, Zn) in the ligand-modified LNA duplexes. *J. Phys. Chem. B 114*, 11942−11948.
(58) Stephenson, K. A., Zubieta, J., Banerjee, S. R., Levadala, M. K., Taggart, L., Ryan, L., McFarlane, N., Boreham, D. R., Maresca, K. P., Babich, J. W., and Valliant, J. F. (2004) A new strategy for the preparation of peptide-targeted radiopharmaceuticals based on an fmoc-lysine-derived single amino acid chelate (SAAC). Automated solid-phase synthesis, NMR characterization, and in vitro screening of fMLF(SAAC)G and fMLF[(SAAC-$Re(CO)_3)^+$]G. *Bioconjugate Chem. 15*, 128−136.
(59) Froidevaux, S., Calame-Christe, M., Schuhmacher, J., Tanner, H., Saffrich, R., Henze, M., and Eberle, A. N. (2004) A gallium-labeled DOTA-α-melanocyte-stimulating hormone analog for PET imaging of melanoma metastases. *J. Nucl. Med. 45*, 116−123.
(60) Allen, G., and Campbell, R. O. (1996) Specific cleavage of histidine-containing peptides by copper (II). *Int. J. Pept. Protein Res. 48*, 265−273.
(61) Mhidia, R., and Melnyk, O. (2010) Selective cleavage of an azaGly peptide bond by copper(II). Long-range effect of histidine residue. *J. Pept. Sci. 16*, 141−147.
(62) Müller, C., Schubiger, P. A., and Schibli, R. (2006) Synthesis and in vitro/in vivo evaluation of novel $^{99m}Tc(CO)_3$-folates. *Bioconjugate Chem. 17*, 797−806.
(63) Banerjee, S. R., Foss, C. A., Castanares, M., Mease, R. C., Byun, Y., Fox, J. J., Hilton, J., Lupold, S. E., Kozikowski, A. P., and Pomper, M. G. (2008) Synthesis and evaluation of technetium-99m- and rhenium-labeled inhibitors of the prostate-specific membrane antigen (PSMA). *J. Med. Chem. 51*, 4504−4517.
(64) Maresca, K. P., Hillier, S. M., Lu, G., Marquis, J. C., Zimmerman, C. N., Eckelman, W. C., Joyal, J. L., and Babich, J. W. (2012) Small molecule inhibitors of PSMA incorporating technetium-99m for imaging prostate cancer: Effects of chelate design on pharmacokinetics. *Inorg. Chim. Acta 389*, 168−175.
(65) King, D. M. (2006) Imaging of metastatic melanoma. *Cancer Imaging 6*, 204−208.
(66) Banerjee, S. R., Pullambhatla, M., Foss, C. A., Falk, A., Byun, Y., Nimmagadda, S., Mease, R. C., and Pomper, M. G. (2013) Effect of chelators on the pharmacokinetics of ^{99m}Tc-labeled imaging agents for the prostate-specific membrane antigen (PSMA). *J. Med. Chem. 56*, 6108−6121.